PLASMA PHYSICS GROUP

Dispersion Discontinuities

of Strong Collisionless Shocks

F. V. Coroniti

March, 1970

R-67

Dispersion Discontinuities of Strong Collisionless Shocks

F. V. Coroniti

March, 1970 R-67

Plasma Physics Group
Department of Physics
University of California
Los Angeles, California
90024

This work was supported in part by the National Science Foundation, Grant # GP 6817; the Office of Naval Research, Grant # NONR-4756(01); the Atomic Energy Commission, Contract AT(11-1)-34, Project #157; and by the National Aeronautics and Space Administration, Contract # NGR-05-007-116.

ABSTRACT

Linear fluid equations are used to estimate wave train properties of strong collisionless shocks. Fast shocks exhibit several dispersion changes with increasing Mach number. For perpendicular propagation into a finite-β plasma, an ion cyclotron radius trailing wave train exists only for $M_F^2 < 2$. Oblique fast shocks have a leading ion inertia wave train if $M_A < \sqrt{M_+/M_-}\cos\theta/2$ and a trailing electron inertia wave train if $M_A > \sqrt{M_+/M_-}\cos\theta/2$. If the downstream sound speed exceeds the flow speed, linear wave theory predicts a trailing ion acoustic structure which probably resides within the magnetic shock. For a turbulent shock model in which an effective electron-ion "collision" frequency exceeds the lower hybrid frequency, ions decouple from the magnetic field; the shock wave train now trails with electron inertia and electron gyroradius lengths. Comparisons of this turbulent model and observations on the earth's bow shock are made.

1.0 Introduction

In the fluid theory of collisionless shocks the transition of macroscopic plasma quantities from a steady upstream to downstream flow state is described by a spatially oscillatory wave train. Oscillation scale lengths are characterized by the natural plasma dispersion lengths, familiar from the theory of linear wave propagation [Stringer, 1963]. Laminar solutions have been applied primarily to weak collisionless shocks, partly because of analytical simplicity and partly because of fundamental difficulties inherent in the fluid formulation [Sagdeev, 1966; Cavaliere and Englemann, 1967]. This paper considers extension of fluid theory into the strong shock regime concentrating exclusively on changes in the wave train dispersive structure. Such restriction permits utilization of linear concepts to obtain qualitative and semi-quantitative estimates of the shock structure.

Fluid shock theories have evolved on two distinct and clearly separable levels: dissipative shocks in which Coulomb interactions control the structure, and dispersive shocks in which collisionless plasma properties dominate. For the present purpose the dissipative limit is instructive since here the structure of strong shocks is reasonably well understood. The transition between allowed Rankine-Hugoniot states occurs over dissipative scale lengths such as the resistive, viscous, or thermal diffusion lengths [Anderson, 1963]. Since dissipation rates vary inversely with thickness, strong shocks, which require intense overall randominzation, often possess a multiply dissipative structure. For example, for fast perpendicular shocks in

which the downstream sound speed exceeds the flow speed, a condition required by the Rankine-Hugoniot relations for upstream Mach numbers exceeding about two, the fluid-magnetic field resistive coupling fails to provide the necessary dissipation. A thin viscous discontinuity or subshock in which the fluid and magnetic field are decoupled and intense viscous dissipation is generated develops within the broader resistive structure [Marshall, 1955; see Fig. 1]. Similar dissipation discontinuities occur in a variety of other fast and slow shock flows [Coroniti, 1970].

In the collisionless limit dissipation processes are assumed sufficiently weak to permit wave dispersion domination of the shock structure. The consistent approximation of weak shocks reduces the complications from nonlinear fluid behavior and allows some confidence in the validity of wave train concepts based on the linear wave theory. Weak collisionless dissipation, such as results from micro-instabilities and three wave decays [Sagdeev, 1966] is usually considered to be driven by the wave train spatial gradients; the total dissipation is accumulated over many wave train oscillations. Hence weak dispersive shock models have generally avoided discontinuities within the wave train structure.

Theoretical considerations of strong collisionless shocks have previously stressed the development of fully turbulent flows in which fluid effects are unimportant [Fishman et al., 1960; Camac et al., 1962; Kennel and Sagdeev, 1967; Tidman, 1967]. Although dissipation again primarily controls the structure, the nonlinear turbulent interactions are so complicated that often no assurance of a complete shock transition in the Rankine-Hugoniot sense is possible; i.e., the downstream state remains unspecified. Therefore, given these difficulties with fully

turbulent shocks, the possibility exists that fluid theory might prove a useful guide to at least some aspects of strong shock structure. Alternatively, strong turbulent dissipation has the tendency of making the plasma behave like a fluid on macroscopic scale lengths; hence some remnants of fluid structure might be expected for strong shocks.

In analogy with multiply dissipative collisional shocks, strong collisionless fluid shocks possibly contain dispersion discontinuities or multiply dispersive wave trains. Strong shocks, however, require strong dissipation. Since plasma turbulent dissipation should be tightly coupled to wave train dispersion gradients, the separation between dispersion and dissipation, which permits great analytical simplification for weak shocks, is considerably more suspect for strong shocks. Recent observations on the earth's collisionless bow shock, however, provide some encouragement for this approach. Fredricks et al. [1970] report that the magnetic shock is often characterized by an electron inertia length wave train-like structure; furthermore, strong electric field wave turbulence, thought to provide considerable ion heating, is coupled to the magnetic field gradients. Hence fluid dispersion remains even in the presence of rapid turbulent dissipation.

The analysis of the nonlinear wave train structure including the self-consistent turbulent dissipation is not yet feasible because of both computational complexity and the absence of a complete theoretical formulation for strong plasma turbulence (see Kellogg [1964] and Bardotti et al. [1967] for some initial efforts). Therefore, the philosophy of this paper is to continue utilization of linear fluid arguments to obtain qualitative estimates on the nonlinear behavior of strong collisionless shocks. In the vicinity of the shock Rankine-Hugoniot

states, wave train amplitudes are small; here the two fluid theory of linear waves can be used to predict dispersion scale lengths and the sign of dispersion, i.e., whether the wave train leads or trails. A concomitant approach is to derive a linearized differential equation for the wave train whose coefficients are then evaluated according to the Rankine-Hugoniot relations. This method is somewhat less useful, however, since a consistent set of fluid equations in differential form which are valid over a wide range of dispersion scale lengths is difficult to formulate. Although the nonlinear structure of the shock center is not realized by these techniques, numerical computations, for restricted shock parameters, have substantiated the general features of the wave train structure predicted by linear theory [Cavaliere and Englemann, 1967].

Section 2.0 reviews the dispersion limitation to the steepening of a finite amplitude compression pulse. Changes in the perpendicular fast shock wave train arising from multiply dispersive wave propagation are considered in terms of the ion acoustic subshock proposed by the Texas group (Robson, 1969) and others (Paul, 1969).

Sections 3.0 and 4.0 discuss fast shock wave trains from several points of view. In Section 3.0 an ion gyroradius length wave train is derived for a finite-β perpendicular shock. For Mach numbers less than two, the predicted shock thickness becomes less than the ion gyroradius, thus violating the small gyroradius expansion of the fluid equations; a speculation on the structure of stronger shocks is presented. The restriction of perpendicular propagation is relaxed in Section 4.0. Oblique fast shocks exhibit a dispersion change from a leading ion inertia to a trailing electron inertia wave train for upstream Alfven Mach numbers exceeding $\sqrt{M_+/M_-}\cos\theta/2$. Finally the ion acoustic subshock

is reconsidered for oblique propagation; restrictions on its occurrence in terms of propagation angle, plasma β, and kinetic theory effects are discussed.

Section 5.0 attempts to simulate the possible effect of a strong turbulent resistivity on the wave train dispersion. If the anomalous collision frequency exceeds the lower hybrid frequency, ions are decoupled from the magnetic field, thus removing ion inertia dispersion even for oblique propagation. The strong shock magnetic structure is then controlled by electron inertia and electron gyroradius dispersion, both of which produce trailing wave trains.

Section 6.0 considers the observations on the earth's bow shock in terms of the previous discussion, and concludes that turbulent resistive decoupling of ions is probably required to explain the electron inertia magnetic wave train. A speculation on the structure of slow shocks predicted to occur in neutral sheet flows is presented.

2.0 Steepening Limitation of Collisionless Shocks

Finite amplitude, long wavelength compression pulses steepen to form shocks [Kantrowitz and Petschek, 1966]. The shock structure is determined by whatever processes limit fluid gradients from becoming arbitrarily large. In collisional shocks, steepening ceases when the pulse width becomes comparable to dissipation scale lengths. In collisionless plasmas steepening limitation arises from linear wave dispersion, which is reviewed here following the arguments of Sagdeev [1966].

As the pulse propagates, nonlinear terms in the fluid equations generate harmonics of the fundamental pulse wave frequency (ω) or wave number (k). If the harmonic-waves also satisfy the same non-dispersive dispersion relation, phase speed ω/k = constant, as the pulse fundamental mode, the pulse propagates as an entity and steepening continues. Hence whenever the small amplitude dispersion relation predicts non-dispersive propagation over some range of ω and k [as in Fig. 2 for $\omega/k = (C_A^2 + C_S^2)^{1/2}$ and $\omega/k = C_S$], compression pulses steepen. As steepening proceeds, however, harmonic modes with wavelengths comparable to plasma dispersion lengths are excited. Typical dispersion lengths are the ion and electron inertial lengths, $C/\omega_{p_\pm}$, the respective particles' gyro-radii, $R_\pm = C_\pm/|\Omega_\pm|$, and the particles Debye lengths, $\lambda_{D_\pm} = C_\pm/\omega_{p_\pm}$. The ± signs refer to ions and electrons, respectively; $\Omega_\pm = \pm eB/M_\pm C$ is the gyro-frequency, B is the magnetic field strength, C is the velocity of light; $\omega_{p_\pm} = (4\pi Ne^2/M_\pm)^{1/2}$ is the specie plasma frequency, N is the number density, e the electronic charge, $M_\pm$ the specie mass; $C_\pm = (T^\pm/M_\pm)^{1/2}$ is the particle thermal speed, and $T^\pm$ is the temperature in energy units. Gaussian units are used throughout.

To illustrate the dispersion limitation of steepening, consider the particular example of the linear fast wave propagating perpendicular to the magnetic field. The dispersion relation when $\beta^{\pm} = 8\pi NT^{\pm}/B^2 < 1$, $T^+/T^- < 1$, and $\omega_{P_+} > |\Omega_+\Omega_-|^{1/2}$ is approximately [Stringer, 1963]

$$\frac{\omega^2}{k^2} = \frac{C_A^2}{1 + (k^2C^2/\omega_{P_-}^2)} + \frac{C_S^2}{1 + k^2\lambda_{D_-}^2} + C_+^2 \left[1 + \frac{T^+}{T^-} \frac{1}{(1 + k^2\lambda_{D_-}^2)} \right] \qquad (2.1)$$

and is sketched in Figs. 2a and 2b. $C_A = (B^2/4\pi NM_+)^{1/2}$ is the Alfven speed and $C_S = (T^-/M_+)^{1/2}$ is the ion acoustic speed. Note that the fast wave is multiply dispersive with both C/ω_{P_-} and λ_{D_-} dispersion lengths. From (2.1) the longest dispersion length attained by the harmonic waves is C/ω_{P_-}; electron inertia decouples the fast wave from the magnetic field and decreases the phase speed below the fast hydromagnetic speed, $\omega/k = (C_A^2 + C_S^2)^{1/2} = C_F$.

Harmonic waves with $kC/\omega_{P_-} \sim 1$, therefore, propagate slower than the pulse and trail behind. Steepening limitation and the formation of a steady state flow is now possible if the compression energy of steepening is removed by wave energy convected out of the pulse. If thermal corrections to (2.1) are neglected, $\beta^{\pm} << 1$, the steady pulse is the magnetic soliton of thickness C/ω_{P_-} [Adlam and Allen, 1958; Sagdeev, 1958; Gardner et al., 1958; Davis et al., 1958]. If the plasma is weakly dissipative, this soliton is converted into a shock wave train [Sagdeev, 1966] consisting of trailing dispersively propagating waves which, in the shock frame, phase stand in the downstream flow. Since, by the steepening limitation arguments, the wave train must convect energy away from the shock, the group velocity of the trailing waves must be less than the phase velocity, $\partial\omega/\partial k < \omega/k$.

From (2.1) note that $\frac{\partial\omega}{\partial k} \sim \frac{\omega}{k} \frac{1}{(1 + k^2C^2/\omega_{p_-}^2)} < \frac{\omega}{k}$ if $\beta^{\pm} << 1$.

Asymptotically downstream the wave train amplitude, having been weakly damped by dissipation, is sufficiently small that the waves approximately obey the linear dispersion relation. Hence an estimate of the wave train oscillation scale length, L , can be obtained by equating the phase speed from (2.1) to the downstream flow speed U_2 predicted by the Rankine-Hugoniot relations. (In Fig. 2a this criterion is satisfied at the intersection of U_2 with the linear dispersion curve, provided, of course, that $\partial\omega/\partial k < \omega/k$ at intersection.) Thermal corrections to (2.1) for this estimate are small if $U_2 > C_{S_2}$ or $\beta_2 < 1$. Performing the calculation yields

$$\frac{L}{2\pi} \sim \frac{C}{\omega_{p_-}} \frac{M_{F_2}}{|M_{F_2}^2 - 1|^{1/2}} \tag{2.2}$$

where the downstream Mach number $M_{F_2} = U_2/C_{F_2}$. The spatial structure of the magnetic wave train is also sketched in Fig. 2a.

When $kC/\omega_{p_-} >> 1$, the fast wave increases its phase velocity to the ion acoustic speed, C_S , and again propagates non-dispersively, $\omega/k \simeq C_S$ until Debye wavelengths are reached; for $k\lambda_D > 1$ the wave slows to the ion thermal speed, C_+. Therefore in the locally non-dispersive region, $\omega/k \simeq C_S$, further shock steepening can occur; indeed when $U_2 < C_{S_2}$, the shock must develop short scale structure at the Debye length since the wave train phase standing condition can only be satisfied by a trailing ion acoustic wave. Note from (2.1) that $\partial\omega/\partial k < \omega/k$ for this wave. On this basis the Texas group [Robson, 1969] has suggested that a general feature of moderately strong collisionless fast shocks is the presence of an ion acoustic subshock. Since the shortest length over

which the magnetic field can change is $C/\omega_{p_-} >> \lambda_{D_-}$, and also since the ion acoustic wave is almost electrostatic [Formisano and Kennel, 1969], the magnetic field is virtually unaffected by the ion acoustic wave train. The subshock acts primarily to slow and heat the ions, and therefore can be considered as the dispersion analogue of the dissipative viscous subshock.

The upstream flow conditions for which an ion acoustic subshock must occur are determined by the perpendicular shock Rankine-Hugoniot relations. Skipping the trivial algebra, C_{S_2}/U_2 as a function of the upstream Mach number M_{F_1} and $\beta_1 = C_{S_1}^2/C_{A_1}^2$, $C_S^2 = 2P/\rho$, is given by

$$\frac{C_{S_2}^2}{U_2^2} = \frac{1}{M_{F_1}^2 + 2}\left[4M_{F_1}^2 - 1 - \frac{27\, M_{F_1}^4}{(M_{F_1}^2+2)^2\,(1+\beta_1)}\right] . \qquad (2.3)$$

Figure 3a is a graph of C_{S_2}/U_2 against M_{F_1} with β_1 as a parameter; Fig. 3b sketches the critical Mach number, M_{crit}, for which $C_{S_2} = U_2$ against β_1. Shocks with $M_{F_1} > 2.5$ have ion acoustic subshocks for any upstream β. The Rankine-Hugoniot relations, Eq. (2.3), actually yield an upper limit to the criteria $U_2 < C_{S_2}$. The wave train will generally have a nonlinear overshoot in the first oscillation [Sagdeev, 1966]; hence in the leading edge $U < C_S$ will occur for lower Mach numbers than given by (2.3). A sketch of an ion acoustic subshock occurring in the leading edge of a C/ω_{p_-} magnetic wave train is included in Fig. 2a.

The oscillation scale length for the ion acoustic wave train can be estimated from the U_2 intersection with the linear dispersion curve. Since for reasonably strong shocks $\beta_2 >> \beta_1$, the dispersion curve differs

from that appropriate to upstream flow conditions; Figure 2b is a sketch of (2.1) for $\beta_2 > 1$. Setting $U_2^2 = \omega^2/k^2 = C_{S_2}^2/(1 + k^2\lambda_{D_-}^2)$, the scale length is

$$\frac{L}{2\pi} \sim \frac{\lambda_{D_-} M_{S_2}}{|1 - M_{S_2}^2|^{1/2}} \tag{2.4}$$

where $M_{S_2} = U_2/C_{S_2}$ and $\lambda_{D_-} \sim C_{S_2}/\omega_{P_{+2}}$. Substituting from (2.3) L becomes

$$\frac{L}{2\pi} \sim \frac{U_1}{\omega_{P_{+1}}} \frac{\sqrt{3}\, M_{F_1}}{(M_{F_1}^2 + 2)^{1/2}} \left[\frac{(4M_{F_1}^2 + 1)(M_{F_1}^2 + 2)^2 - [27M_{F_1}^4/(1+\beta_1)]}{3(M_{F_1}^2 - 1)(M_{F_1}^2 + 2)^2 - [27M_{F_1}^4/(1+\beta_1)]} \right] . \tag{2.5}$$

In summary, this section has established the following points on the utilization of linear fluid theory to determine wave train structure:

a) Hydromagnetic compression pulses steepen in regions of non-dispersive linear wave propagation.

b) Steepening is limited at pulse thicknesses comparable to dispersion scale lengths. Wave trains are formed by dispersively propagating waves which phase stand in the downstream flow and have $\partial\omega/\partial k < \omega/k$, or in the upstream flow with $\partial\omega/\partial k > \omega/k$.

c) Wave train scale lengths can be estimated by matching linear wave phase speeds to flow speeds at the asymptotic Rankine-Hugoniot states. Linear dispersion curves appropriate to upstream or downstream Rankine-Hugoniot conditions must be used for these estimates.

c) Since the linear dispersion relation is multiply dispersive, perpendicular fast shocks possess a magnetic wave train with C/ω_{P_-} lengths, and for $M_{F_1} > M_{crit}$, an ion acoustic subshock at Debye lengths. Because

of the wave train nonlinear overshoot, the Rankine-Hugoniot relations provide an upper limit on M_{crit}. Since it interacts primarily with ions leaving the magnetic field unaffected, the ion acoustic subshock is the dispersion analogue of the viscous subshock.

3.0 The Perpendicular Ion Cyclotron Radius Wave Train

In the previous section the discussion of the perpendicular fast shock was restricted to consideration of only electron inertia and Debye length dispersion. As this shock steepens in a finite-β^+ plasma, however, the longest dispersion length encountered is the ion cyclotron radius (ICR). In Section 3.1 an ICR wave train differential equation is derived for the linear perturbed plasma response about the asymptotic stationary flows. For moderate Mach numbers the shock steepens to lengths shorter than R_+ thus passing beyond the validity of the fluid analysis. Kinetic theory effects and steepening to shorter scale lengths are discussed.

3.1 Derivation of the ICR Wave Train Differential Equation

To investigate the perpendicular ICR fast shock wave train, the analysis employs the Chew-Goldberger-Low hydromagnetic equations with first order ICR corrections as derived by MacMahon [1965]. (A similar approach has been used by Kinsinger and Auer, 1969; Goldberg, 1970.) The range of validity for these equations requires $\beta^+ >> M_-/M_+$, assuring $R_+ >> C/\omega_{p_-}$, $T^+/T^- >> (M_-/M_+)^2$ so that $R_+ >> R_-$ and $\Omega_+/\omega_{p_+} << 1$ or $R_+ >> \lambda_{D_+}$, thus restricting consideration to quasi-neutral plasmas. In addition, only shock scale lengths $L >> R_+$ can be treated, consistent with the first order ICR expansion of the fluid equations. The wave train structure is investigated only about the upstream and downstream stationary Rankine-Hugoniot flows, thus permitting a linearized analysis. This method examines the stability at the stationary points of the nonlinear wave train differential equation; shock transition requires instability upstream and stability downstream.

The coordinate system in the steady shock frame, used throughout this paper, is specified by shock propagation in the X-direction, along which plasma quantities vary, with the magnetic field, B_z, in the Z-direction. The perturbed time independent fluid equations are

$$\rho U \delta U + \delta P_{xx}^{(1)} + \frac{B_z \delta B_z}{4\pi} = \mu \frac{d\,\delta U}{dx} \tag{3.1}$$

$$\rho U\, \delta V_y + \delta P_{xy}^{(1)} = \eta \frac{d\,\delta V_y}{dx} \tag{3.2}$$

$$\rho U^2\, \delta U + U(\delta P_{\perp}^{(1)} + \delta P_{xx}^{(1)}) + P_{\perp}^{(1)}\, \delta U + U \frac{\delta P_{\parallel}^{(1)}}{2} + \frac{P_{\parallel}^{(1)}}{2} \delta U$$

$$+ (\delta \underset{\sim}{q}_{\perp}^{\perp(1)} + \delta \underset{\sim}{q}_{\perp}^{\parallel(1)}) \cdot \hat{x} + \frac{U_1 B_{z_1} \delta B_z}{4\pi} = \mu U \frac{d\,\delta U}{dx} \tag{3.3}$$

$$U\, \delta B_z + B_z\, \delta U = 0 \tag{3.4}$$

$$\delta(U \frac{P_{\parallel}^{(1)}}{2} + \underset{\sim}{q}_{\perp}^{\parallel(1)} \cdot \hat{x}) = 0 \tag{3.5}$$

$$\delta P_{xx}^{(1)} = \delta P_{\perp}^{(1)} - \frac{P_{\perp}^{(0)+}}{2\Omega_+} \frac{d\,\delta V_y}{dx} \tag{3.6}$$

$$\delta P_{xy}^{(1)} = \frac{P_{\perp}^{(0)+}}{2\Omega_+} \frac{d\,\delta U}{dx} \tag{3.7}$$

$$\delta \underset{\sim}{q}_{\perp}^{\perp(1)} \cdot \hat{x} = \frac{2P_{\perp}^{(0)+}}{NM_+\Omega_+} \frac{d\,\delta P_{xy}^{(1)}}{dx} \tag{3.8}$$

Following the notation of MacMahon [1965], superscripts (0) and (1) denote zero and first order quantities, respectively, in the small ICR expansion. $\perp$ ($\parallel$) denotes perpendicular (parallel) to the magnetic field. δ denotes a perturbed variable; the unperturbed quantities are to be evaluated about either the upstream, subscript (1), or downstream,

subscript (2), flow conditions. U is the flow velocity in the X-direction; V_y is the fluid velocity in the transverse Y-direction. P, appropriately sub- and super-scripted, denotes the pressure. $\delta q_{\perp}^{(1)} \cdot \hat{x}$ and $\delta q_{\perp}^{u(1)} \cdot \hat{x}$ are the first order ICR heat flows along X, and are retained since they contribute to the same order as the pressure tensor ICR terms in the energy equation (3.3); zero order heat flow has been neglected. Effective viscosity coefficients, η, ζ, and $\mu = \frac{4}{3}\eta + \zeta$ are included to simulate weak collisional or turbulent dissipation.

Neglecting products of ICR and viscosity terms, the above equations reduce to a wave train differential equation for δU

$$\frac{3}{4} R_+^2 \frac{d^2 \delta U}{dx^2} + \frac{\mu U}{P_{\perp}^{(0)+}} \frac{d \delta U}{dx} - \frac{U^2 - C_F^2}{P_{\perp}^{(0)+}/\rho} \delta U = 0 \qquad (3.9)$$

$R_+ = (P_{\perp}^{(0)+}/\rho\Omega_+^2)^{1/2}$ is the ion cyclotron radius, and $C_F = [C_A^2 + (2P_{\perp}^{(1)}/\rho)]^{1/2}$ is the fast hydromagnetic speed. Solutions of (3.9) in the form $\exp(\lambda x)$ are

$$\lambda = \frac{-\mu U}{\frac{3}{2} P_{\perp}^{(0)+} R_+^2} \pm \frac{1}{R_+} \left[\frac{U^2 - C_F^2}{\frac{3}{4} P_{\perp}^{(0)+}/\rho} \right]^{1/2} \qquad (3.10)$$

where terms proportional to μ^2 have been neglected. About the upstream flow U exceeds C_F by the shock evolutionary conditions [Kantrowitz and Petschek, 1966]; (3.10) then yields δU exponentially increasing (corresponding to U slowing down) with a scale length

$$L \sim \left[\frac{3}{4} \frac{P_{\perp 1}^{(0)+}}{\rho_1 C_{F_1}^2} \right]^{1/2} \frac{R_+}{(M_{F_1}^2 - 1)^{1/2}} \qquad (3.11)$$

where $M_{F_1} = U_1/C_{F_1}$. About the downstream flow, $U_2 < C_{F_2}$, and (3.10)

yields a damped trailing ICR wave train, as predicted by MacMahon [1968], and Fredricks and Kennel [1968].

The above wave train analysis is valid as long as the small ICR expansion of the Chew-Goldberger-Low fluid equations is preserved. For weak shocks, $M_{F_1}^2 - 1 \ll 1$, (3.11) predicts $L \gg R_+$; hence the ICR dispersive wave train should resolve the shock structure. If $M_{F_1}^2 - 1 > \frac{3}{4} (P_\perp^{(0)+}/\rho_1 C_{F_1}^2) < 1$, $L < R_+$ and the above fluid analysis breaks down.

3.2 Discussion

A qualitative understanding of the wave train structure for stronger shocks is obtainable by considering the linear dispersion relation for the perpendicular magnetosonic wave. A collisionless kinetic Vlasov treatment of the full electromagnetic perpendicular dispersion relation has been performed by Fredricks [1968]; the result is summarized in Fig. 4. The kinetic theory predicts electromagnetic cut-offs ($k \to 0$) and electrostatic resonances ($k \to \infty$) at harmonics of the ion cyclotron frequency; also note the approximate resonance at the lower hybrid frequency. The envelopes along the maximum group velocity points of each dispersion curve are lines given by $\omega/k = C_F$ and $\omega/k = C_S$.

Now consider, as in Section 2.0, the predictions of the fast shock wave train structure implied by Fig. 4. First note that no upstream wave trains are possible since, at the intersections of U_1 with the dispersion curves, $\partial\omega/\partial k \simeq 0$, and energy would be convected into, not out of, the shock. The downstream flow speed intersects the curves at all cyclotron harmonics, and here the group velocity condition for trailing wave trains is satisfied. Hence, naively, the kinetic theory predicts a wave train

with a multiplicity of discrete oscillation lengths corresponding to each harmonic of Ω_+ .

Several difficulties with the above arguments are apparent. First, a finite Coulomb or anomalous collision frequency, which must be present in the downstream shock flow, would tend to destroy to fine scale ion harmonic structure; hence collisionless kinetic theory probably poorly approximates the fluid behavior of the plasma. Second, consider a pulse with thickness of order R_+ or less which is undergoing steepening along the approximately non-dispersive part, $\omega/k \simeq C_F$, of the dispersion curves in Fig. 4. Since the ions traverse the pulse width only once ($U > C_+$), the nonlinearly excited waves associated with steepening do not sense the full ion gyro-coupling to the magnetic field. To these waves the ion orbits appear almost as straight lines; hence ion harmonic dispersive structure given by the kinetic theory for infinite plane waves cannot effectively limit the steepening of narrow compression pulses. The waves generated by steepening should approximately obey the two fluid dispersion relation of Stringer [1963] and Formisano and Kennel [1969], and remain non-dispersive until electron inertia slows down the fast wave at frequencies near the lower hybrid. From Section 2.0, the shock structure is a trailing C/ω_{p_-} wave train. Note that the maximum group velocity envelopes including the dispersion of electron inertia at the lower hybrid frequency in Fig. 4 approximates the two fluid dispersion curves in Figs. 2a and 2b.

In summary, for weak perpendicular fast shocks $M_{F_1}^2 - 1 << \frac{3}{4}(P_\perp^{(0)+}/\rho C_F^2)$, $L >> R_+$, and the ICR trailing wave train derived from the Chew-Goldberger-Low hydromagnetic equations with first order ICR corrections probably describes the shock structure reasonably well. For stronger shocks, ICR dispersion fails to limit steepening; steepening continues until a C/ω_{p_-}

or possibly λ_D wave train is formed. Finally, even though only perpendicular propagation has been considered, the ineffectiveness or weakness of ICR dispersion to limit strong fast shock steepening probably also holds for oblique strong shocks. Hence in the following sections ICR dispersion will be neglected.

4.0 Oblique Fast Shocks

If the restriction of perpendicular propagation is relaxed, ion inertia dispersion becomes competitive with electron inertia for angles $\theta > \pi/2 - \sqrt{M_-/M_+}$. The Mach number dependence of this transition is discussed in Section 4.1 using the linear dispersion relation. Section 4.2 reconsiders the ion acoustic subshock for oblique propagation; high-β and kinetic theory effects are also discussed.

4.1 Oblique Magnetic Fast Shocks

Since the wave train differential equation for the whistler shock has been extensively analyzed by several authors [see Sagdeev, 1966; Cavaliere and Englemann, 1967], the two fluid linear whistler dispersion relation will be employed here to determine the wave train structure. The strong shock limit is stressed.

If $|\Omega_-|/\omega_{p_-} \ll 1$, the phase speed of the fast wave is approximately given by [Stringer, 1963; Formisano and Kennel, 1969],

$$\frac{\omega^2}{k^2} = \frac{k^2C^2}{\omega_{p_+}^2}\,\frac{C_A^{\,2}\cos^2\theta}{(1 + k^2C^2/\omega_{p_-}^2)^2} + \frac{C_A^{\,2}}{1 + k^2C^2/\omega_{p_-}^2} + \frac{C_S^{\,2}\sin^2\theta}{1 + k^2\lambda_{D_-}^2}$$

$$+ C_+^{\,2}\left[1 + \frac{T^+}{T^-}\,\frac{1}{(1 + k^2\lambda_{D_-}^2)}\right] \qquad (4.1)$$

where θ is the angle between the flow velocity and the magnetic field direction. Figure 5 is a sketch of ω/k against k ; intersections of ω/k with possible upstream, U_1 and U_1' , and downstream, U_2 and U_2' ,

flow speeds are included. In order to clearly separate magnetic and temperature effects in (4.1), $\beta^{\pm}$ is taken somewhat less than unity so that in the range $k = 0$ to $k\lambda_{D_-} < 1$, the first two terms in (4.1) dominate the dispersion relation. Note that since for strong shocks ICR dispersion was neglected in (4.1), β^{+} is not restricted to be $< M_-/M_+$ as in the calculations of Cavaliere and Englemann [1967].

If $\theta > \pi/2 - \sqrt{M_-/M_+}$, ion inertia dispersion, C/ω_{P_+}, in the first term of (4.1) exceeds that of electron inertia and increases the fast wave phase speed above the hydromagnetic speed, C_F. At the first intersection of U_1 with the dispersion curve, the whistler stands in the upstream flow and forms a leading wave train. Note from (4.1) that $\partial\omega/\partial k > \omega/k$ if $kC/\omega_{P_-} \ll 1$; hence wave energy propagates upstream out of the shock. The oscillation length, found by setting $\omega/k = U_1$, neglecting C/ω_{P_-} terms, and solving (4.1) for k, is given by

$$\frac{L}{2\pi} \sim \frac{\cos\theta_1}{(M_{A_1}^2 - 1)^{1/2}} \frac{C}{\omega_{P_+}} \tag{4.2}$$

where $M_{A_1} = U_1/C_{A_1}$, the Alfven Mach number. The magnetic wave train is also sketched in Fig. 5.

From (5.1) the maximum whistler phase velocity is $\omega/k = (C_a \cos\theta)/2$, attained when $kC/\omega_{P_-} = 1$; $C_a = (B^2/4\pi NM_-)^{1/2}$. Therefore the maximum upstream Alfven Mach number for which the whistler forms a leading wave train is $M_{A_1} = \sqrt{M_+/M_-}\,(\cos\theta_1/2)$; the scale length is $L \sim 2\pi\,(C/\omega_{P_-})$.

For $U_1 > (C_{a_1} \cos\theta_1)/2$, the only wave train possible is at the interaction of the downstream flow speed. (The second U_1 intersection is disallowed since, $\partial\omega/\partial k < \omega/k$, energy would be blown back into the shock.) If $U_2 > C_{S_2}$, which probably restricts $M_{A_1} < 2$ to 3 or

$\cos\theta_1 < (2 \text{ to } 3) \times 2\sqrt{M_-/M_+}$, the linear dispersion relation predicts a trailing magnetic wave train. The scale length, obtained by solving (4.1) for k and taking the root of the bi-quadratic for $U_2 < (C_{a_2} \cos\theta_2)/2$, is approximately

$$\frac{L}{2\pi} \sim \sqrt{\frac{M_-}{M_+}} \; \frac{M_{A_2}}{\cos\theta_2} \; \frac{C}{\omega_{P_-}} \tag{4.3}$$

or $L \lesssim \pi(C/\omega_{P_-})$.

For stronger shocks, $U_1 > (C_{a_1} \cos\theta_1)/2 > (2 \text{ to } 3) \times C_A$, $U_2 < C_{S_2}$. Furthermore, even if $U_1 < (C_{a_1} \cos\theta_1)/2$ so that a C/ω_{P_+} wave train leads, $U_2 < C_{S_2}$ can occur. In previous magnetic wave train analysis crossing of the downstream sonic point corresponds to what has been called the breaking of the wave train [Cavaliere and Englemann, 1967; see also Section 5.0]. Note that the sonic point can occur locally in the wave train and need not always occur at the asymptotic downstream flow; nonlinear overshoots can also give $U = C_S$ locally. A collisional or turbulent ion viscosity, or the ion acoustic subshock wave train is required for a complete shock transition. However, since reduction of U to C_S must be accomplished by magnetic and density compression, the magnetic shock structure should be approximately that predicted by wave trains. For the C/ω_{P_+} wave train, many leading oscillations are probably necessary for $U < C_S$ to occur locally in the shock (see Fig. 5). In the trailing wave train U probably decreases through C_S in the leading edge (see Fig. 2). The initial magnetic gradient should possess a C/ω_{P_-} characteristic length [Sagdeev, 1966]. Since the ions are decoupled from the magnetic field at the sonic point, whether or not a complete or even a partial C/ω_{P_-} wave train exits downstream is unclear; further analytical or numerical work is necessary to resolve this difficulty.

In summary, for low Mach numbers $M_{A_1} < \sqrt{M_+/M_-}\ \cos\theta_1/2$, the shock structure is a leading ion inertia wave train. For stronger shocks, a dispersion change to a shorter scale length occurs; the wave train now trails and has an electron inertia length. If $U = C_S$ anywhere in the shock flow, a dissipation (viscous subshock) or dispersion (ion acoustic subshock) discontinuity results; structure of magnetic wave trains for $U < C_S$ is unclear.

4.2 Oblique Ion Acoustic Subshock

Whether or not an ion acoustic subshock occurs for oblique shock flows depends on the downstream propagation angle θ_2 and the plasma β. The fast shock evolutionary conditions require that $U_2 \geq C_{I_2} = C_{A_2}\cos\theta_2$, the intermediate speed [Kantrowitz and Petschek, 1966]; hence for $\beta_2 < 1$, $U_2 < C_{S_2}$ results only if $\theta_2 > \cos^{-1}(C_{S_2}/C_{A_2})$. For moderately strong shocks, $M_{F_1} > 2$ to 3, however, β_2 probably exceeds unity so that $U_2 < C_{S_2}$ occurs at all propagation angles.

An additional constraint on the appearance of an ion acoustic subshock is that β_1 or $\beta_2 < (M_+/M_-)(\cos^2\theta/2)$, since at higher pressures the maximum whistler phase speed $\omega/k = C_a\cos\theta/2 < C_S$; if $\theta = \pi/2$, this constraint becomes $\beta < \sqrt{M_+/M_-}$. Here the dispersion relation (4.1) no longer describes the fast wave but becomes the intermediate wave dispersion relation if the last two terms are dropped; for $\beta > (M_+/M_-)(\cos^2\theta/2)$, the fast mode is approximately an isotropic ion acoustic wave and remains non-dispersive up to $k\lambda_D \sim 1$ [Formisano and Kennel, 1969]. The ion acoustic wave train is now just the electrostatic shock derived by Moiseev and Sagdeev [1963] in the $\beta \to \infty$ limit.

A further consideration on the occurrence of the ion acoustic subshock

is the relation of U_2 to the ion thermal speed, C_+. Figure 6 for $\omega_{p_+} > |\Omega_-|\cos\theta$ and Fig. 7 for $|\Omega_-|\cos\theta > \omega_{p_+}$ are sketches of the dispersion curves for the three quasi-hydromagnetic waves which propagate below the electron plasma frequency [Stringer, 1963]; the curves are drawn for $\cos\theta < C_S/C_A$, $\beta^{\pm} < 1$, and $C_+ > C_I$. If $\beta > 1$, Figs. 6 and 7 are modified by moving the sonic line C_S closer to the C_F line, thus reducing the region of C/ω_{p_-} dominance in the dispersion relation. Note that in the vicinity of $k\lambda_D \sim 1$, if $\omega_{p_+} > |\Omega_-|\cos\theta$, the fast wave first speeds up to C_S and then slows to C_+. If $|\Omega_-|\cos\theta > \omega_{p_+}$, the intermediate wave, which is an isotropic sound wave for $kC/\omega_{p_+} \gg 1$ and $k\lambda_D \ll 1$, slows to C_+ and then intersects the fast mode near $\omega \sim |\Omega_-|\cos\theta$; the fast wave passes non-dispersively through C_S and then speeds up to C_+.

Two points merit discussion. First, for the fast shock to steepen to an ion acoustic subshock, the linear fast wave dispersion relation must possess a non-dispersive region with $\omega/k \simeq C_S$. Therefore from Fig. 6, only shocks in plasmas with $\omega_{p_+} > |\Omega_-|\cos\theta$ or $\omega_{p_+} > |\Omega_+\Omega_-|^{1/2}$ if $\theta = \pi/2$ have ion acoustic subshocks. Second, the downstream flow speed for $M_F \gg 1$ is constrained by the Rankine-Hugoniot relations to be at least $\gtrsim \frac{1}{4} U_1$, but the temperature jump across the shock has $T_2 \to \infty$ for $M_F \to \infty$ [Anderson, 1963]; hence $U_2 \sim C_+$ is possible for strong shocks. The fluid dispersion curves in Figs. 2, 6, and 7, are non-dispersive for $\omega/k = C_+$, and further shock steepening might be thought possible. However, the kinetic theory predicts heavy ion Landau damping when $\omega/k = C_+$ [Stix, 1962], so that whether the waves with $\omega/k \sim C_+$ generated by nonlinear steepening can propagate is extremely doubtful. Furthermore the ion acoustic wave is also ion Landau damped unless $T^-/T^+ \gg 1$. Therefore the ion acoustic subshock is likely to occur only if

$\omega_{P_+} > |\Omega_-|\cos\theta$ or $|\Omega_+\Omega_-|^{1/2}$, $C_S \gtrsim U_2 \gg C_+$ and $T^-/T^+ \gg 1$. Strong shock flows violating these criteria probably have fully turbulent structures, although possibly in conjunction with a magnetic wave train.

4.3 Discussion

The fast shock wave train structure exhibits three dispersion changes or discontinuities with increasing shock strength. For $\theta = \pi/2$ and $M_{F_1}^2 - 1 > \frac{3}{4}(P_\perp^{(0)+}/\rho C_F^2)$ ICR dispersion ceases to inhibit shock steepening, and short scale length C/ω_{P_-} or λ_{D_-} wave trains develop; if $\theta \neq \pi/2$ and $\beta^+ > 1$ so that $R_+ > C/\omega_{P_+}$, a magnetic ion inertia wave train is also possible. The whistler magnetic wave train changes from leading with C/ω_{P_+} to a trailing with C/ω_{P_-} lengths when $M_{A_1} > \sqrt{M_+/M_-}\cos\theta/2$. Finally for $M_F > 2$ to 3, $U_2 < C_{S_2}$, and the ion acoustic subshock proposed by the Texas group is possible if $C_{S_2} > U_2 \gg C_+$, $\omega_{P_+} > |\Omega_-|\cos\theta$ or $|\Omega_+\Omega_-|^{1/2}$ and $T^-/T^+ \gg 1$.

5.0 Strong Turbulence Modification of Wave Train Dispersion

In plasmas where the Coulomb collision mean free path greatly exceeds even the longest dispersion scale lengths, collisionless plasma turbulence must provide the necessary shock dissipation. Collisionless turbulence often requires strong gradients, either in Cartesian or velocity space, as sources of unstable free energy [Sagdeev and Galeev, 1969]. In addition to whatever background turbulence exists in the flow, wave train gradients, especially in strong shocks, should generate intense turbulent dissipation. Wave dispersion properties, and hence wave train scale lengths, however, may be modified by strong turbulence. In this section this dissipation modification is illustrated, albeit not self-consistently, by a model shock flow in which an effective or turbulent electron-ion collision frequency, ν_{eff}, exceeds the lower hybrid frequency $\Omega_{LH} = |\Omega_+\Omega_-|^{1/2}$. Note that the usual two fluid equations require $\nu_{eff} << \Omega_{LH}$ [see Cavaliere and Englemann, 1967]. Since ions are now effectively decoupled from the magnetic field by collisions, ion inertia and ICR dispersion will not limit shock steepening or form wave trains; hence the shock wave train structure should be controlled by electron dispersion.

To obtain further insight on the collisional suppression of ion dispersion, consider the cold plasma oblique fast shock wave train analysis of Cavaliere and Englemann [1967]. The ratio of the growth or dissipative length, L_g, of the leading ion inertia wave train to the dispersion scale length L was found to be

$$\frac{L_g}{L} = \frac{(U/\nu_{eff})\ [\cos^2\theta/M_A^2(M_A^2-1)]\ (M_+/M_-)}{[\cos\theta/(M_A^2-1)^{1/2}]\ (C/\omega_{P_+})} = \frac{\Omega_{LH}}{\nu_{eff}}\ \frac{\cos\theta\ \sqrt{M_+/M_-}}{M_A(M_A^2-1)^{1/2}} \qquad (5.1)$$

From the discussion of Section 4.1, the maximum value of $(\cos\theta\ \sqrt{M_+/M_-})/M_A$ for ion inertia dispersion to dominate the wave train is 2; hence the growth length becomes shorter than the dispersion length if $\nu_{eff}/\Omega_{LH} \gtrsim 2/(M_A^2-1)^{1/2}$. Therefore for sufficiently strong shocks, $M_A^2-1 >> 1$, and $\nu_{eff} \gtrsim \Omega_{LH}$ ion inertia scale length effects are suppressed by collisions, and the wave train structure must be controlled by electron dispersion. Weak shocks under the above conditions are probably adequately described by hydromagnetics. ICR dispersion is eliminated if $\nu_{eff} > \Omega_+$ since, by the usual arguments leading to the MHD equations, the ion pressure tensor will be approximately isotropic.

The equations describing the strong shock electron dispersion structure are the exact conservation relations for the fluid mass, momentum, and energy, which, if viscosity is neglected, do not involve the dissipation directly, and Ohm's law, which describes the interaction of the fluid and magnetic field including dissipation. In two fluid theory Ohm's law correct to order M_-/M_+ can be written

$$M_- \frac{d}{dt}(\underline{V}^+ - \underline{V}^-) = e\left[\underline{E} + \frac{\underline{V}\times\underline{B}}{C}\right] - M_+ \frac{d\underline{V}}{dt} - \frac{1}{N}\nabla\cdot\underline{\underline{P}}^+ - \frac{M_-\nu_{eff}\underline{J}}{Ne} \qquad (5.2)$$

$\underline{V}$ is the fluid velocity, $\underline{V}^{\pm}$ the specific particle velocity, $J = Ne(\underline{V}^+ - \underline{V}^-)$ the current density, and $\underline{E}$ the electric field.

To formulate Ohm's law consistent with $\nu_{eff} > \Omega_{LH}$, Eq. (5.2) must be ordered. Since electrons, because of their small inertia, carry the predominant part of the current, $\underline{J} \sim -Ne\,\underline{V}^-$. If the current carrying

electron velocity $\underline{V}^-$ is of order $\sqrt{M_+/M_-}\,\underline{V}^+$ and $E \sim V^+B/C$, the terms in (5.2) can be ordered as

$$\frac{1}{\Omega_{LH}\tau} = 1 : 1 : \frac{1}{\Omega_+\tau} : \frac{1}{\Omega_+\tau} : \frac{\nu_{eff}}{\Omega_{LH}} \tag{5.3}$$

or

$$\sqrt{M_-/M_+} = \Omega_+\tau : \Omega_+\tau : 1 : 1 : \sqrt{M_-/M_+}\,\nu_{eff}\,\tau \tag{5.4}$$

where τ is the time required to go a scale length $\tau \sim L/U$. On electron inertia scale lengths $\tau \sim C/\omega_{p_-} U \sim M_A/\Omega_{LH}$; hence $\Omega_+\tau \sim \sqrt{M_-/M_+} \ll 1$. Therefore from (5.4) and (5.2) consistency requires that over short electron dispersion lengths

$$NM_+ \frac{dV}{dt} + \nabla\cdot\underset{\approx}{P}^+ \approx 0 \tag{5.5}$$

and

$$M_- \frac{d}{dt}(\underline{V}^+ - \underline{V}^-) = e\left[\underline{E} + \frac{\underline{V}\times\underline{B}}{C}\right] - \frac{M_-\nu_{eff}\underline{J}}{Ne} \quad . \tag{5.6}$$

Since the mass velocity $\underline{V} \sim \underline{V}^+$, (5.5) predicts that the ion motion is decoupled from the magnetic field, i.e., the ions obey hydrodynamics. Furthermore (5.5) coupled with the momentum equation implies that

$$\frac{\underline{J}\times\underline{B}}{C} - \nabla\cdot\underset{\approx}{P}^- \approx 0 \tag{5.7}$$

or that on C/ω_{p_-} scale lengths, current forces are balanced primarily by electron pressure gradients. In (5.6), which replaces the full Ohm's law, the only scale length which appears is electron inertia. The ordering condition $\Omega_{LH}L/U < 1$, however, requires that the flow scale length, $L \sim U/\Omega_{LH} \sim C/\omega_{p_-} \sim \beta_-^{-1/2} R_-$; hence if $\beta^- \sim 1$, electron cyclotron radius (ECR) corrections must be included in the wave train analysis.

The wave train will again be investigated by considering only the linear response about the asymptotic stationary flow. To further simplify the calculation, the ion pressure tensor is taken isotropic, and the electron parallel and perpendicular pressures are assumed equal, both probably reasonable due to the high collision frequency; ECR corrections to $\underset{\sim}{P}$ are retained, however. In addition, only very oblique fast shocks are treated so that $\cos\theta = B_x/B \ll 1$, although θ is not restricted in the range $\frac{\pi}{2} - \sqrt{M_-/M_+} < \theta < \frac{\pi}{2}$; consequently $U \ll C_I = C_A \cos\theta$ also holds. With these approximations the perturbed fluid equations neglecting viscosity and zero order heat flow are

$$\rho U\, \delta U + \delta P_{xx}^{(1)} + \frac{B_z\, \delta B_z}{4\pi} = 0 \tag{5.8}$$

$$\rho U\, \delta V_y + \delta P_{xy}^{(1)} - \frac{B_x\, \delta B_y}{4\pi} = 0 \tag{5.9}$$

$$\rho U\, \delta V_z + \delta P_{xz}^{(1)} - \frac{B_x\, \delta B_z}{4\pi} = 0 \tag{5.10}$$

$$\rho U[U\delta U + V_z \delta V_z] + \frac{3}{2}\,(U\delta P^{(1)} + P^{(1)}\,\delta U) + U\delta P_{xx}^{(1)} + P_{xx}^{(1)}\,\delta U + V_z \delta P_{xz}^{(1)} + \frac{U_1 B_{z_1}\, \delta B_z}{4\pi} + (\delta \underline{q}_{\perp}^{(1)} + \delta \underline{q}_{\perp}^{u(1)}) \cdot \hat{x} = 0 \tag{5.11}$$

$$\frac{C^2}{\omega_{P_-}^2} U \frac{d^2 \delta B_z}{dx^2} + \frac{C^2}{\omega_{P_-}^2} \nu_{eff} \frac{d\delta B_z}{dx} = U\delta B_z + B_z \delta U - B_x \delta V_z \tag{5.12}$$

$$\frac{C^2}{\omega_{P_-}^2} U \frac{d^2 \delta B_y}{dx^2} + \frac{C^2}{\omega_{P_-}^2} \nu_{eff} \frac{d\delta B_y}{dx} = U\delta B_y - B_x \delta V_y \tag{5.13}$$

$$U_1 B_{z_1} = U B_z - [B_x{}^2 (B_z - B_{z_1})]/4\pi\rho U \tag{5.14}$$

$$\delta P_{xx}^{(1)} = \delta P^{(1)} + \frac{P^{(0)-}}{2|\Omega_-|} \frac{B_z}{B} \frac{d\delta V_y^-}{dx} \tag{5.15}$$

$$\delta P_{xy}^{(1)} = - \frac{P^{(0)-}}{2|\Omega_-|} \frac{B_z}{B} \frac{d\delta U^-}{dx} \tag{5.16}$$

$$\delta P_{xz}^{(1)} = \frac{P^{(0)-}}{2|\Omega_-|} \frac{B_x B_z^2}{B^3} \frac{d\delta V_y^-}{dx} \tag{5.17}$$

$$(\delta \underline{q}_{\perp}^{(1)} + \delta \underline{q}_{\perp}^{u(1)}) \cdot \hat{x} = \frac{5}{4} \frac{(P^{(0)-})^2}{NM_-|\Omega_-|^2} \frac{B_z^2}{B^2} \frac{d^2\delta U^-}{dx^2} \tag{5.18}$$

$$\delta V_y^- = \frac{C}{4\pi Ne} \frac{d\delta B_z}{dx} \tag{5.19}$$

$$\delta V_z = - \frac{C}{4\pi Ne} \frac{d\delta B_y}{dx} \tag{5.20}$$

$$U^- = U ; \qquad \delta U^- = \delta U \quad . \tag{5.21}$$

In the above equations $V_y = B_y = 0$ at the Rankine-Hugoniot stationary points was used.

Equations (5.8) through (5.21) are straightforwardly reduced to a pair of wave train differential equations for δB_z and δB_y except for the elimination of δU from (5.18). Since (5.18) is an ECR term, presumed small, and by the assumption of $U >> C_I$, a sufficient approximation, in (5.18) only, is to take $\delta U \approx - (U/B_z)\, \delta B_z$. The results are

$$\frac{C^2}{\omega_{P_-}^2} \frac{d^2\delta B_z}{dx^2} + \frac{\frac{5}{3}(P^{(0)-}/\rho)(B_z^2/B^2) + (B_z^2/4\pi\rho)}{U^2 - C_S^2} R_-^2 \frac{d^2\delta B_z}{dx^2} + \frac{C^2}{\omega_{P_-}^2} \frac{\nu_{eff}}{U} \frac{d\delta B_z}{dx} =$$

$$= \frac{(U^2-C_F^2)(U^2-C_{SL}^2)}{U^2(U^2-C_S^2)} \delta B_z \tag{5.22}$$

$$\frac{C^2}{\omega_{P_-}^2}\,\frac{d^2\delta B_y}{dx^2} + \frac{C^2}{\omega_{P_-}^2}\,\frac{\nu_{eff}}{U}\,\frac{d\delta B_y}{dx} = \frac{U^2 - C_I^2}{U^2}\,\delta B_y \tag{5.23}$$

where $R_-^2 = P^{(0)-}/2|\Omega_-|^2 NM_-$ is the electron cyclotron radius; C_F and C_{SL} are the fast and slow hydromagnetic speeds defined by

$$\left.\begin{matrix} C_F^2 \\ C_{SL}^2 \end{matrix}\right\} = \frac{C_A^2 + C_S^2}{2} \pm \left[\left(\frac{C_A^2 + C_S^2}{2}\right)^2 - C_A^2\,C_S^2\cos^2\theta\right]^{1/2} \tag{5.24}$$

Note that δB_z and δB_y are decoupled, a consequence of the very oblique approximation.

Solutions of (5.22) describe an exponential rise in B_z at the leading edge of the shock and a trailing $C/\omega_{P_-} - R_-$ wave train, each with a scale length given approximately by

$$L \sim \frac{\left[\dfrac{C^2}{\omega_{P_-}^2} + \dfrac{\frac{5}{3}\,(P^{(0)-}/\rho)\,(B_z^2/B^2) + (B_z^2/4\pi\rho)}{U^2 - C_S^2}\,R_-^2\right]^{1/2}}{[(C_F^2|M_F^2-1|)/(U^2-C_S^2)]^{1/2}} \tag{5.25}$$

where L is to be evaluated at the upstream or downstream flow conditions, respectively. The damping length for the trailing wave train is

$$L_D \sim \frac{2\left[\dfrac{C^2}{\omega_{P_-}^2} + \dfrac{\frac{5}{3}\,(P^{(0)-}/\rho)\,(B_z^2/B^2) + (B_z^2/4\pi\rho)}{U^2 - C_S^2}\,R_-^2\right]^{1/2}}{(C^2/\omega_{P_-}^2)\;(\nu_{eff}/U)} \tag{5.26}$$

evaluated for downstream conditions. Note that the familiar wave train "breaking" occurs when $U < C_S$ since the pseudo-potential term on the

right hand side of (5.22) changes sign and L becomes imaginary. Either a turbulent viscosity or a Debye length ion acoustic subshock is required to further describe the downstream shock structure. Equation (5.23) does not yield a complete shock transition for B_y, and probably just represents the damped rotational intermediate wave which is decoupled from the fast wave when ion inertia dispersion is neglected. Hence the magnetic shock should be primarily compressive.

The above analysis is undoubtedly a poor approximation to the ion dynamics since changes of the ion fluid on either long, C/ω_{p_+}, R_+, or very short, λ_D, scale lengths are not included. The shock structure observed in the magnetic field and electron fluid, however, should be reasonably well described by the $C/\omega_{p_-} - R_-$ trailing wave train up to, and maybe also beyond, the sonic point.

In summary, if strong plasma turbulence creates an effective collision frequency $\nu_{eff} > \Omega_{LH}$, only electrons couple to the magnetic field and provide magnetic dispersion. Strong fast shocks have a $C/\omega_{p_-} - R_-$ trailing magnetic wave train. Although the above calculation was restricted to very oblique fast shocks, the qualitative features of the wave train structure are probably valid for a larger range of propagation angles. Furthermore note that $M_A > \sqrt{M_+/M_-}\cos\theta/2$ was not required to obtain a $C/\omega_{p_-} - R_-$ scale length wave train.

6.0 Discussion

6.1 Summary

By use of essentially linear arguments the following estimates on the wave train structure of fast shocks have been derived:

a) Weak perpendicular finite-β shocks, $M_F^2 - 1 < \frac{3}{4}\left(P_\perp^{(0)+}/\rho C_F^2\right) < 1$, have a trailing R_+ wave train. For stronger shocks, probably including oblique propagation, ICR dispersion does not limit steepening; wave trains for both $\beta < 1$ and $\beta > 1$ will not involve R_+ scale lengths.

b) Oblique magnetic whistler shocks have leading ion inertia wave trains if $M_{A_1} < \sqrt{M_+/M_-}\ \cos\theta_1/2$ and trailing electron inertia wave trains if $M_{A_1} > \sqrt{M_+/M_-}\ \cos\theta_1/2$.

c) When $M_{F_1} > 2$ to 3, the Debye length trailing ion acoustic subshock proposed by the Texas group occurs if $\beta < (M_+/M_-)(\cos^2\theta/2)$ and $\omega_{p_+} > |\Omega_-|\cos\theta$, or for $\theta = \pi/2$, $\beta < \sqrt{M_+/M_-}$ and $\omega_{p_+} > \Omega_{LH}$, $C_{S_2} > U_2 >> C_+$, and $T^-/T^+ >> 1$. As in its dissipation analogue, the viscous subshock, the ion acoustic subshock decouples the fluid from the magnetic field and acts primarily to heat the ions without affecting the magnetic shock structure.

d) Strong turbulent dissipation modifies plasma dispersion characteristics. For $\nu_{eff} > \Omega_{LH}$ and strong fast shocks, ions are decoupled from the magnetic field and magnetic wave trains trail with $C/\omega_{p_-} - R_-$ scale lengths. Here numerical computations [Kellogg, 1964; Bardotti, et al., 1966] are necessary to treat the turbulence generated by wave train gradients self-consistently.

The fluid arguments suggesting that strong shocks might have short scale length wave trains are probably somewhat oversimplified. In uniform plasmas short wavelength oblique linear waves are often heavily Landau or cyclotron damped. Therefore in order for a shock to steepen into a short dispersion length wave train, the nonlinear excitation or growth rate of these modes must exceed the linear, and possibly nonlinear, damping rates. Failure to do so may constitute a criterion for the development of a fully turbulent strong shock. It should be noted that Debye length wave trains for an electrostatic ion acoustic shock have been observed in the laboratory [Taylor, et al., 1970]. Furthermore short C/ω_{p_-} magnetic scale lengths have been observed in the earth's bow shock.

6.2 The Earth's Bow Shock

Although laminar low Mach number shocks have been studied in the laboratory for many years [Paul, et al., 1965; Kurtmullaev, et al., 1966; Robeson, et al., 1968], high Mach number, high-β collisionless shocks are presently accessible only in space plasmas. The bow shock formed by the interaction of the super-magnetosonic solar wind with the earth's magnetosphere has recently been probed by the high telemetry rate satellite OGO-5 [Fredricks, et al., 1968]. Although highly variable, the shocks examined by Fredricks, et al., [1970] are often characterized by: (see Fig. 8)

1. A magnetic field precursor with scale lengths $\sim C/\omega_{p_-}$;

2. a large magnetic jump followed by several oscillations both with gradients $\sim C/\omega_{p_-}$;

3. large amplitude electrostatic turbulence with frequencies $\sim \omega_{p_+}$ which maximize at the C/ω_{p_-} gradients in the magnetic field and are

thought to be generated by either the ion acoustic or Bunemann current instabilities;

4. rapid proton thermalization occurring in regions where the electrostatic wave amplitudes maximize.

Theoretically, the most puzzling aspect of these shock observations is what appears to be a C/ω_{p_-} trailing wave train in the magnetic field. For typical solar wind flow conditions, $M_A \sim 4\text{-}10$, $\beta^{\pm} \sim 1$, $\theta \neq \pi/2$, the criteria for a C/ω_{p_-} dispersion discontinuity discussed in Sections 4.1 ($M_A > \sqrt{M_+/M_-}\cos\theta/2$) and 3.1 ($\theta = \pi/2$, $M_F \gtrsim 1.5$) are generally not satisfied, although exceptions almost certainly occur. Hence on the basis of phase standing arguments ion inertia should dominate the longest scale length wave train.

A possible explanation of the C/ω_{p_-} scale length is the turbulent dissipation modification of plasma dispersion characteristics. For the current driven electrostatic turbulence observed in the shock precursor and wave train structure, Sagdeev [1965] has estimated the effective collision frequency as $\nu_{eff} \simeq \omega_{p_+}/10$. In the bow shock $B \sim 10^{-4}$ gauss and $N \sim 10$ cm^{-3}, $\omega_{p_+}/10\Omega_{LH} \sim 10$; hence, by the arguments of Section 5.0, the ions should be decoupled from the magnetic field, and the magnetic wave train should be characterized by the electron dispersion lengths $C/\omega_{p_-} - R_-$. Ion turbulent decoupling might commence in the precursor, thus permitting a $C/\omega_{p_-} - R_-$ wave train in the center of the shock, or it might be a feature of the solar wind. Recently Forsland [1970] has investigated electron heat flow "current" instabilities in the solar wind as a means of turbulently heating ions. If the dissipation rate from these instabilities is also of order $\omega_{p_+}/10$, the ion fluid behaves hydrodynamically in the solar wind; the electron fluid then carries the magnetic field and provides the only magnetic wave train dispersion lengths.

6.3 Slow Shocks in Neutral Sheet Flows

A popular hypothesis in space and cosmological physics is that magnetic energy can be rapidly converted into particle and flow energy at x-type neutral points [Levy et al., 1964; Axford et al., 1965; Sturrock, 1967]. Petschek [1964] and Petschek and Thorne [1967] have proposed a hydromagnetic flow in which most of the magnetic field annihilation occurs across standing slow shocks bounding the neutral sheet. It is somewhat disturbing that although the neutral sheet in the tail of the magnetosphere has been probed by many satellites, no direct evidence of the predicted slow shocks has been found. Furthermore typical neutral sheet thicknesses are quite thin, $\sim$ 600 km [Ness, 1965] or on the order of C/ω_{P_+} or R_+. Therefore if slow shocks indeed exist in the tail of the magnetosphere, an ordinary two-fluid hydromagnetic model for slow shocks, which would predict shock thicknesses C/ω_{P_+} or R_+, appears to be inadequate to account for the observed thin neutral sheets.

To obtain rapid magnetic field annihilation in collisionless slow shocks requires a large turbulent resistivity which probably can only be provided by ion acoustic or Bunemann current instabilities driven by steep magnetic field gradients. A reasonable speculation is that if the turbulent collision frequency satisfies $\nu_{eff} > \Omega_{LH}$, the slow shock structure is dominated by short scale length electron dispersion with the ion fluid decoupled from the magnetic field (Section 5.0). If the ECR term is neglected, Eq. (5.22) also describes a low-β oblique slow shock wave train. At the leading edge B_z decreases exponentially with a scale length

$$L \sim \frac{C_S}{C_F} \frac{M_{SL}}{|M_{SL}^2-1|^{1/2}} \frac{C}{\omega_{P_-}} \tag{6.1}$$

where $M_{SL} = U/C_{SL}$; downstream the wave train trails with a wavelength given by (6.1) evaluated about the downstream flow. Of course, if $\beta^- \gtrsim 1$, ECR corrections to (6.1) must be included; the ECR term in (5.22) is incorrect for slow shocks since terms of order B_x^2/B^2 have been dropped. In the tail of the magnetosphere $C/\omega_p \sim 5$ km so that a complete slow shock wave train could easily reside within the "thin" neutral sheets observed by satellites.

Acknowledgments

It is a pleasure to acknowledge many useful and illuminating discussions with Professors C. F. Kennel and W. B. Kunkel. This work also benefited from many conversations with Drs. R. W. Fredricks and F. L. Scarf.

This work was supported in part by NASA Grant NGR 05-007-190 and the National Science Foundation.

References

Adlam, J. H., and J. E. Allen, Proc. 2nd U. N. International Conference on Peaceful Uses of Atomic Energy, 221, 1958.

Anderson, J. E., Magnetohydrodynamic Shock Waves, M.I.T. Press, 1963.

Axford, W. I., H. E. Petschek, and G. L. Siscoe, J. Geophys. Res. 70, 1231 (1965).

Bardotti, G., A. Cavaliere, and F. Englemann, Nuclear Fusion 6, 46, 1966.

Camac, M., A. R. Kantrowitz, M. M. Litvak, R. M. Patrick, and H. E. Petschek, Nucl. Fusion Suppl., Part 2, 423, 1962.

Cavaliere, A., and F. Englemann, Nucl. Fusion, 7, 137, 1967.

Coroniti, F. V., J. Plasma Phys., 1970.

Davis, L., R. Lust, and A. Schluter, Z. Naturforsch., 13a, 916, 1958.

Fishman, F. J., A. R. Kantrowitz, and H. E. Petschek, Rev. Mod. Phys., 32, 959, 1960.

Formisano, V., and C. F. Kennel, J. Plasma Phys., 3, 55, 1969.

Forsland, P. W., J. Geophys. Res., 75, 17, 1970.

Fredricks, R. W., C. F. Kennel, F. L. Scarf, G. M. Crook, and I. M. Green, Phys. Rev. Letters, 21, 1761, 1968.

Fredricks, R. W., and C. F. Kennel, J. Geophys. Res., 73, 7429, 1968.

Fredricks, R. W., J. Plasma Physics, 2, 365, 1968.

Fredricks, R. W., G. M. Crook, C. F. Kennel, I. M. Green, F. L. Scarf, P. J. Coleman, and C. T. Russel, J. Geophys. Res., 1970.

Gardner, C. S., H. Goertzel, H. Grad, C. S. Morawitz, M. H. Rose, and H. Rubins, Proc. 2nd U. N. International Conference on Peaceful Uses of Atomic Energy, 31, 230, 1958.

Goldberg, P., Phys. Fluids, 1970

Kantrowitz, A. R. , and H. E. Petschek, in Plasma Physics in Theory and Application, ed. by W. B. Kunkel, 148, McGraw-Hill Book Co., New York, 1966.

Kellogg, P. J., Phys. Fluids 7, 1555, 1964.

Kennel, C. F., and R. Z. Sagdeev, J. Geophys. Res. 72, 3303, 1967.

Kinsinger, R. E., and P. L. Auer, Phys. Fluids, 12, 2580, 1969.

Kurtmullaev, R. K., Yu. E. Nesterikhin, V. I. Pilsky, and R. Z. Sagdeev, in Plasma Physics and Controlled Thermonuclear Fusion, Vol. 2, 367, IAEA Vienna, 1966.

Levy, R. H., H. E. Petschek, and G. L. Siscoe, AIAA J., 2, 2065, 1964.

MacMahon, A., Phys. Fluids, 8, 1840, 1965.

MacMahon, A., J. Geophys. Res. 73, 7538, 1968.

Marshall, W., Proc. Roy. Soc., London, A232, 367, 1955.

Moiseev, S. S., andR. Z. Sagdeev, Plasma Phys. (J. Nucl. Energy, Part C) 5, 43, 1963.

Ness, M. F., J. Geophys. Res. 70, 2989, 1965.

Paul, J. W. M., in Collision-Free Shocks in the Laboratory and Space, ESRO SP - 51, 97, Dec. 1969.

Paul, J. M. W., L. S. Holmes, M. J. Parkinson, and J. Sheffield, Nature 208, 133, 1965.

Petschek, H. E., in Proc. AAS-NASA Symp. Phys. Solar Flares, NASA SP-50, ed. by W. N. Hess, 425, Washington, D. C., 1964.

Petschek, H. E., and R. M. Thorne, Astrophys. J., 147, 1157, 1967.

Robson, A. E., in Collision-Free Shocks in the Laboratory and Space, ESRO SP-51 159, Dec. 1969.

Robson, A. E., J. Sheffield, and R. J. Bickerton, Bull. Am. Phys. Soc., 13, 293, 1968.

Sagdeev, R. Z., Plasma Physics and the Problem of Controlled Thermonuclear Research, Vol. 5, 454, 1958.

Sagdeev, R. Z., Annual Symposium on Applied Mathematics, Courant Institute, New York University, 1965.

Sagdeev, R. Z., in Reviews of Plasma Physics, Vol. 4, 23, Consultants Bureau, New York, 1966.

Sagdeev, R. Z., and A. A. Galeev, Nonlinear Plasma Theory, W. A. Benjamin, New York, 1969.

Stix, T. H., The Theory of Plasma Waves, McGraw-Hill, New York, 1962.

Stringer, T. E., Plasma Phys. (J. Nucl. Energy, Part C), 5, 89, 1963.

Sturrock, P., Proc. of the International School of Physics, Enrico Fermi Course XXXIX, Academic Press, New York, 1967.

Taylor, R. J., D. R. Baker, and H. Ikezi, Phys. Rev. Letters, 24, 206, 1970.

Tidman, D. A., Phys. Fluids, 10, 547, 1967.

Figure Captions

Figure 1.

Sketch of the shock structure in velocity and magnetic field for a collision dominated hydromagnetic perpendicular fast shock. The magnetic shock is characterized by the magnetic Reynolds length $r_m = C^2/4\pi\sigma U$, where σ is the conductivity based on electron-ion collisions. If $U_2 < C_{S_2}$, a viscous subshock occurs in the downstream flow; ion-ion collisions slow and heat the plasma across the viscous Reynolds length $r_e = \mu/\rho U$, where μ is the coefficient of viscosity.

Figures 2a and 2b.

The perpendicular fast linear wave dispersion relation, ω vs. k, is sketched for $\omega_{P_+} > |\Omega_+\Omega_-|^{1/2}$ and for $\beta^{\pm} << 1$ (Fig. 2a) and $\beta^{\pm} > 1$ (Fig. 2b). Possible intersections of the downstream flow speed U_2 with the dispersion curves are included. Shock steepening occurs in locally non-dispersive regions, $\omega/k = (C_A^2 + C_S^2)^{1/2} = C_F$ and $\omega/k = C_S$; steepening is limited by dispersively propagating waves with $kC/\omega_{P_-} \sim 1$ or $k\lambda_{D_-} \sim 1$. The magnetic shock is described by a C/ω_{P_-} length trailing wave train. If $U_2 < C_{S_2}$, U_2 intersects the dispersion curve near $k\lambda_{D_-} \sim 1$; an electrostatic Debye length ion acoustic wave train occurs in the flow velocity and temperature, but probably not in the magnetic field. For reasonably strong shocks, $M_F^2 - 1 \sim 1$ or for $\beta_1^{\pm} \sim 1$, the appropriate dispersion curve for estimating wave train scale lengths is Fig. 2b; note that the region over which C/ω_{P_-} dominates wave dispersion is reduced.

Figures 3a and 3b.

The ratio of the downstream sound speed to flow speed, C_{S_2}/U_2, as determined by the Rankine-Hugoniot relations for a perpendicular fast shock is plotted in 3a against upstream Mach number M_F, with β_1 as a parameter. In 3b the critical upstream Mach number, M_{crit}, for which $U_2 = C_{S_2}$ is plotted against β_1. An ion acoustic or viscous subshock results when $U_2 < C_{S_2}$; for $M_{F_1} > 2.5$, $U_2 < C_{S_2}$ for all upstream β's.

Figure 4.

The perpendicular fast wave dispersion relation as determined by Fredricks [1968] from kinetic theory using the full Maxwell equations is sketched. Electromagnetic cut-offs ($k \to 0$) and electrostatic resonances ($k \to \infty$) occur at harmonics of the ion cyclotron frequency, $n\Omega_+$. The envelopes of the maximum group velocity points on each harmonic branch are given by the lines $\omega/k = C_F$ and $\omega/k = C_S$. Note the approximate resonance at the lower hybrid frequency, Ω_{LH}, sketched here to lie between $(n+1)\,\Omega_+$ and $(n+2)\Omega_+$.

Figure 5.

A sketch of ω/k against k for the oblique whistler dispersion relation. Ion inertia dispersion, C/ω_{P_+}, increases the phase velocity up to the $\omega/k = C_a \cos\theta/2$; electron inertia dispersion, C/ω_{P_-}, then decouples the wave from the magnetic field and decreases ω/k to C_S. Debye length dispersion, λ_D, further reduces ω/k to the ion thermal speed C_+. If the upstream flow speed U_1 intersects the dispersion curve near $kC/\omega_{P_+} \sim 1$, the magnetic shock structure is a leading C/ω_{P_+} wave train. For $U_1 > C_a \cos\theta/2$ no waves stand upstream, and the magnetic

shock has a short scale $< C/\omega_{P_-}$ trailing wave train. If $U < C_S$ occurs locally somewhere in the shock flow, the velocity and temperature have an ion acoustic subshock wave train with λ_D lengths.

Figure 6.

A sketch of the three quasi-hydromagnetic waves which propagate below the electron plasma frequency [see Stringer, 1963]. The dispersion curves are drawn for $\omega_{P_+} > |\Omega_-| \cos\theta$, $\beta \lesssim 1$, and $C_S > C_I > C_+$. Near $k\lambda_D \sim 1$, the fast wave phase speed first increases to C_S and then decreases to C_+.

Figure 7.

Same as Fig. 6 except that $|\Omega_-| \cos\theta > \omega_{P_+}$. The intermediate wave, $\omega/k = C_S$ for $kC/\omega_{P_+} \gg 1$, decreases its phase speed to C_+ near $k\lambda_D \sim 1$ and then intersects the fast branch at $\omega \sim |\Omega| \cos\theta$. The fast wave passes non-dispersively through C_S, and then speeds up to C_+.

Figure 8.

Data from a single crossing of the earth's bow shock on March 12, 1968, as observed by OGO-V [Fredricks, et al., 1970]. The first graph is the total magnetic field $|\underline{B}|$ in units of 10^{-5} Gauss. A short wavelength, $\sim C/\omega_{P_-}$, magnetic precursor leads the major increase in the field strength; a wave train-like series of oscillations with scale lengths again $\sim C/\omega_{P_-}$ trail in the downstream flow. The second graph is the ion flux, J_+, from the Lockheed ion spectrometer. Ion thermalization occurs at the magnetic jump. The third graph is the AC electric field spectral amplitudes plotted against frequency; the numbers correspond to those in the first graph of $|\underline{B}|$. The maximum electric field amplitudes occur at the maximum gradient of $|\underline{B}|$.

Multiply dissipative perpendicular fast shock with viscous subshock

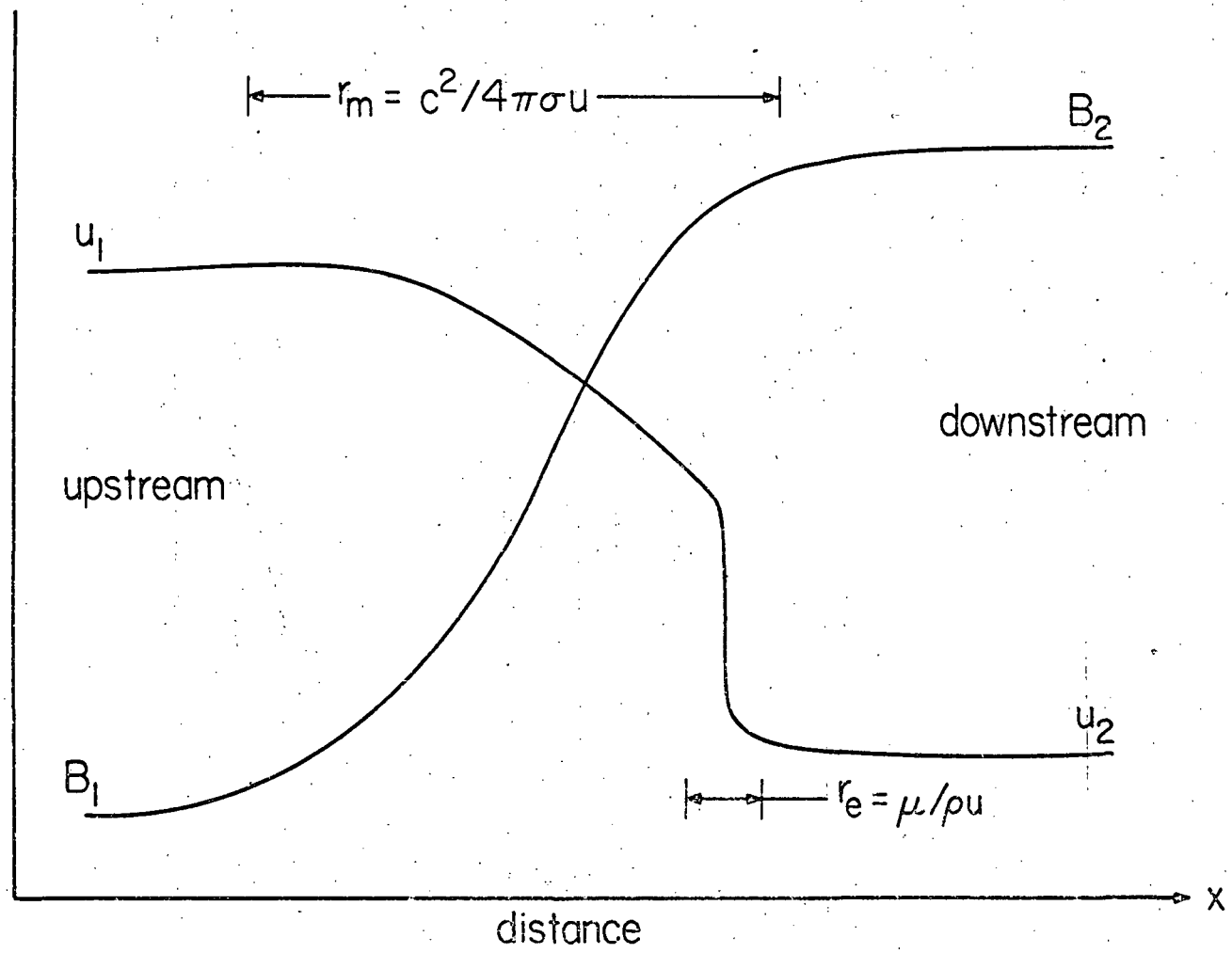

Figure 1

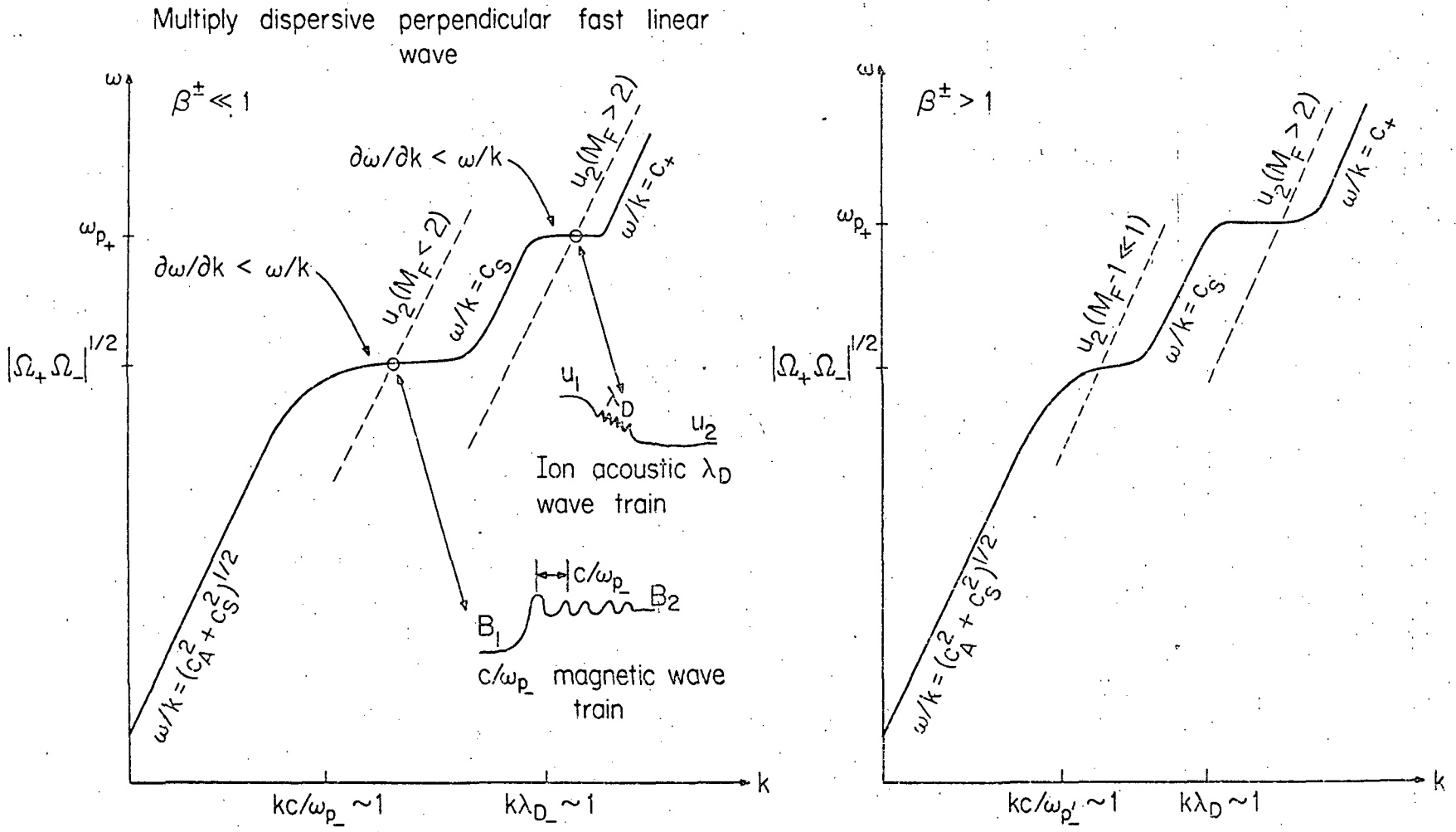
Multiply dispersive perpendicular fast linear wave
$\beta^{\pm} \ll 1$
ω
ω_{p_+}
$|\Omega_+ \Omega_-|^{1/2}$
$\partial\omega/\partial k < \omega/k$
$u_2(M_F < 2)$
$\omega/k = c_S$
$\partial\omega/\partial k < \omega/k$
$u_2(M_F > 2)$
$\omega/k = c_+$
u_1
λ_D
u_2
Ion acoustic λ_D wave train
c/ω_{p_-}
B_2
B_1
c/ω_{p_-} magnetic wave train
$\omega/k = (c_A^2 + c_S^2)^{1/2}$
k
$kc/\omega_{p_-} \sim 1$
$k\lambda_{D_-} \sim 1$
$\beta^{\pm} > 1$
ω
ω_{p_+}
$|\Omega_+ \Omega_-|^{1/2}$
$u_2(M_F - 1 \ll 1)$
$\omega/k = c_S$
$u_2(M_F > 2)$
$\omega/k = c_+$
$\omega/k = (c_A^2 + c_S^2)^{1/2}$
k
$kc/\omega_{p_-} \sim 1$
$k\lambda_D \sim 1$

Figure 2

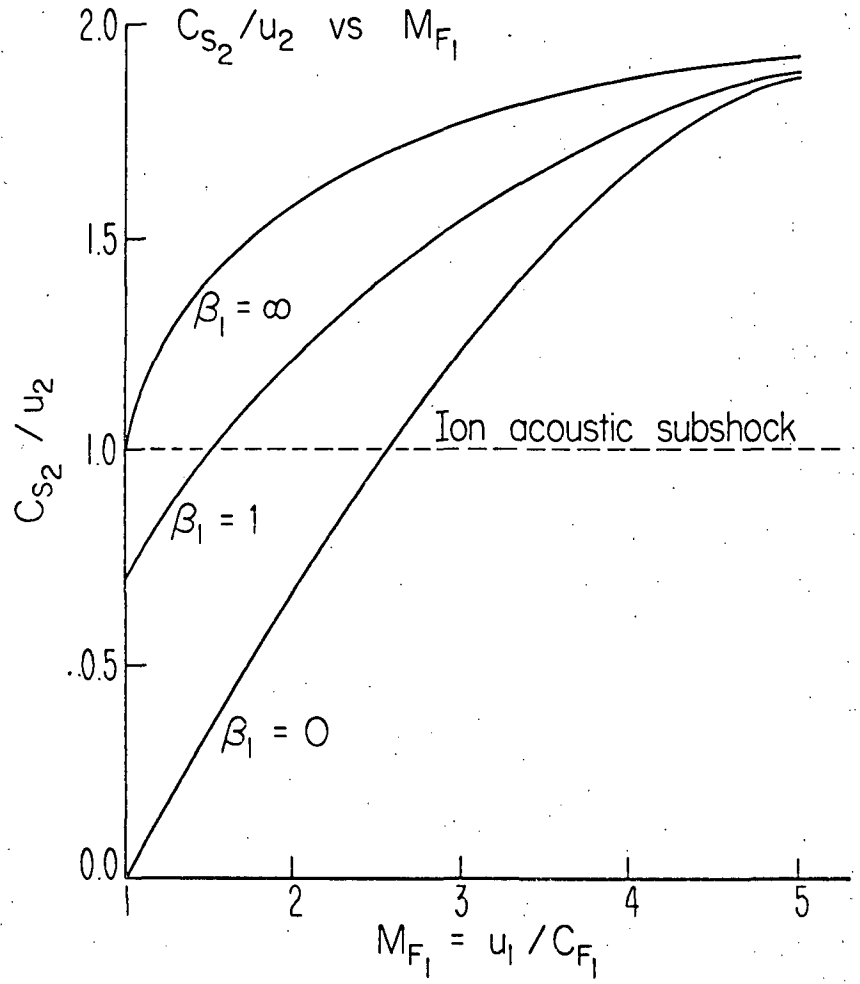
C_{S_2}/u_2 vs M_{F_1}
2.0
1.5
1.0
.0.5
0.0
C_{S_2}/u_2
$\beta_1 = \infty$
$\beta_1 = 1$
$\beta_1 = 0$
Ion acoustic subshock
1
2
3
4
5
$M_{F_1} = u_1 / C_{F_1}$

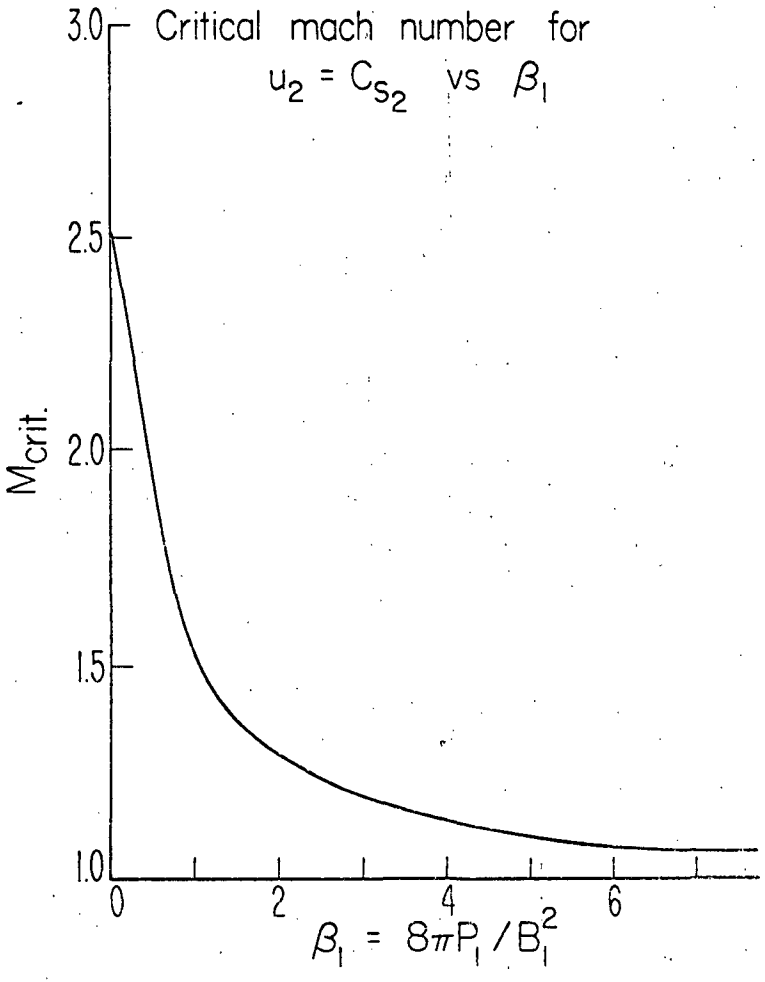
Critical mach number for
$u_2 = C_{S_2}$ vs β_1
3.0
2.5
2.0
1.5
1.0
$M_{crit.}$
0
2
4
6
$\beta_1 = 8\pi P_1 / B_1^2$

Figure 3

Perpendicular fast wave with kinetic theory ion harmonic structure

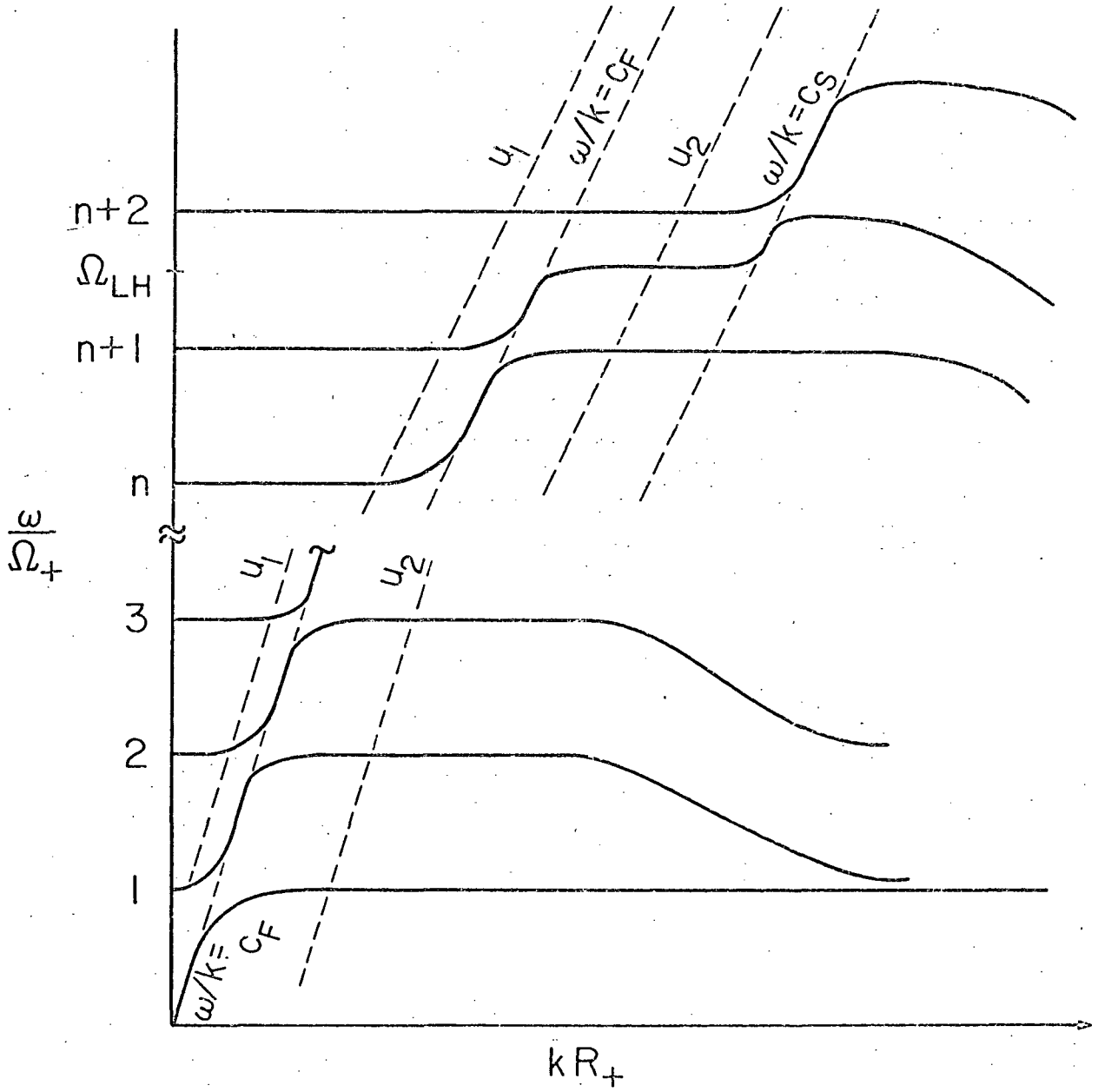

Figure 4

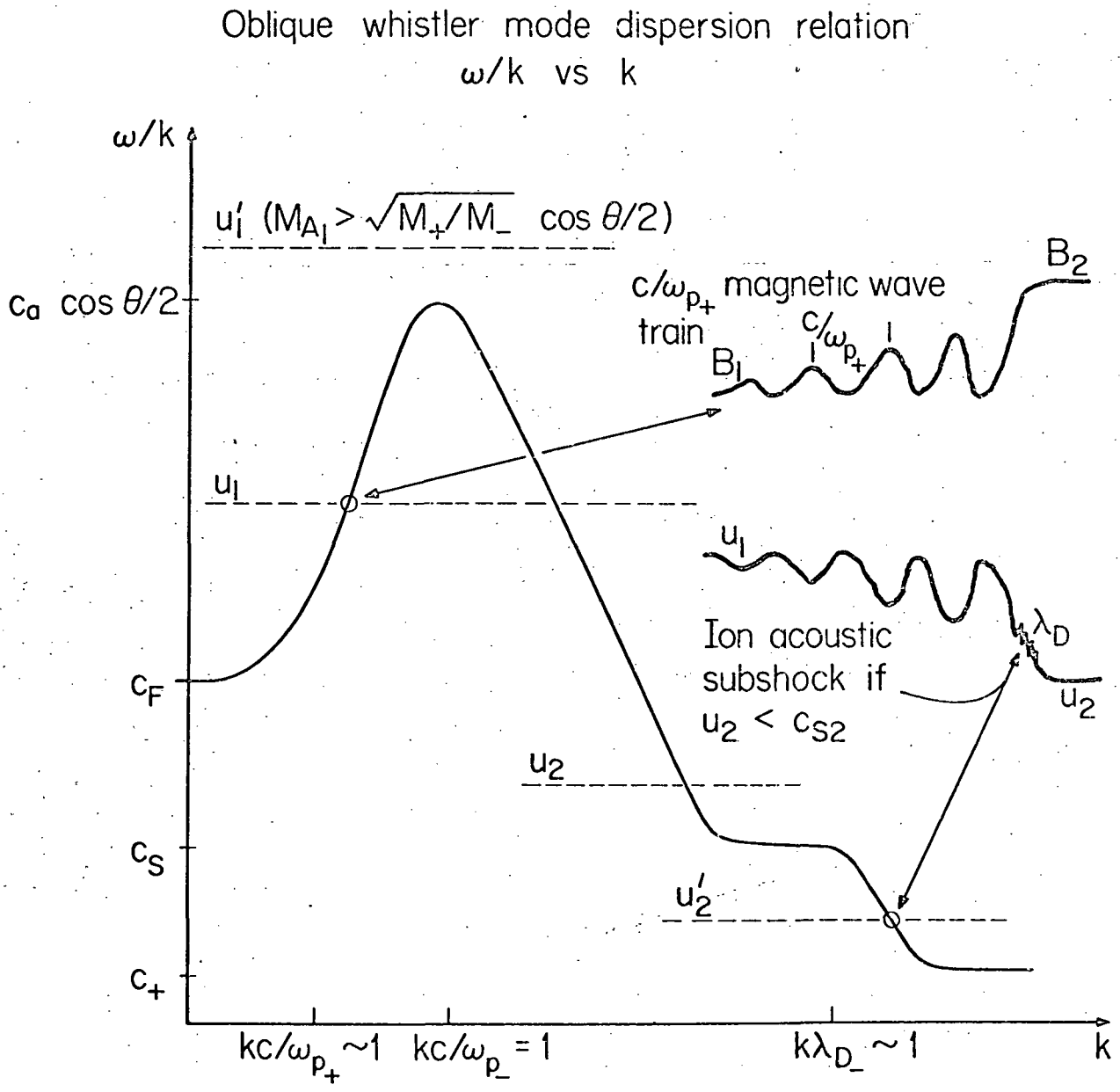
Oblique whistler mode dispersion relation
ω/k vs k
ω/k
u_1' ($M_{A_1} > \sqrt{M_+/M_-}\cos\theta/2$)
$c_a \cos\theta/2$
c/ω_{p_+} magnetic wave train
B_2
B_1
c/ω_{p_+}
u_1
u_1
λ_D
Ion acoustic subshock if $u_2 < c_{S2}$
u_2
u_2
c_F
c_S
u_2'
c_+
$kc/\omega_{p_+} \sim 1$
$kc/\omega_{p_-} = 1$
$k\lambda_{D_-} \sim 1$
k

Figure 5

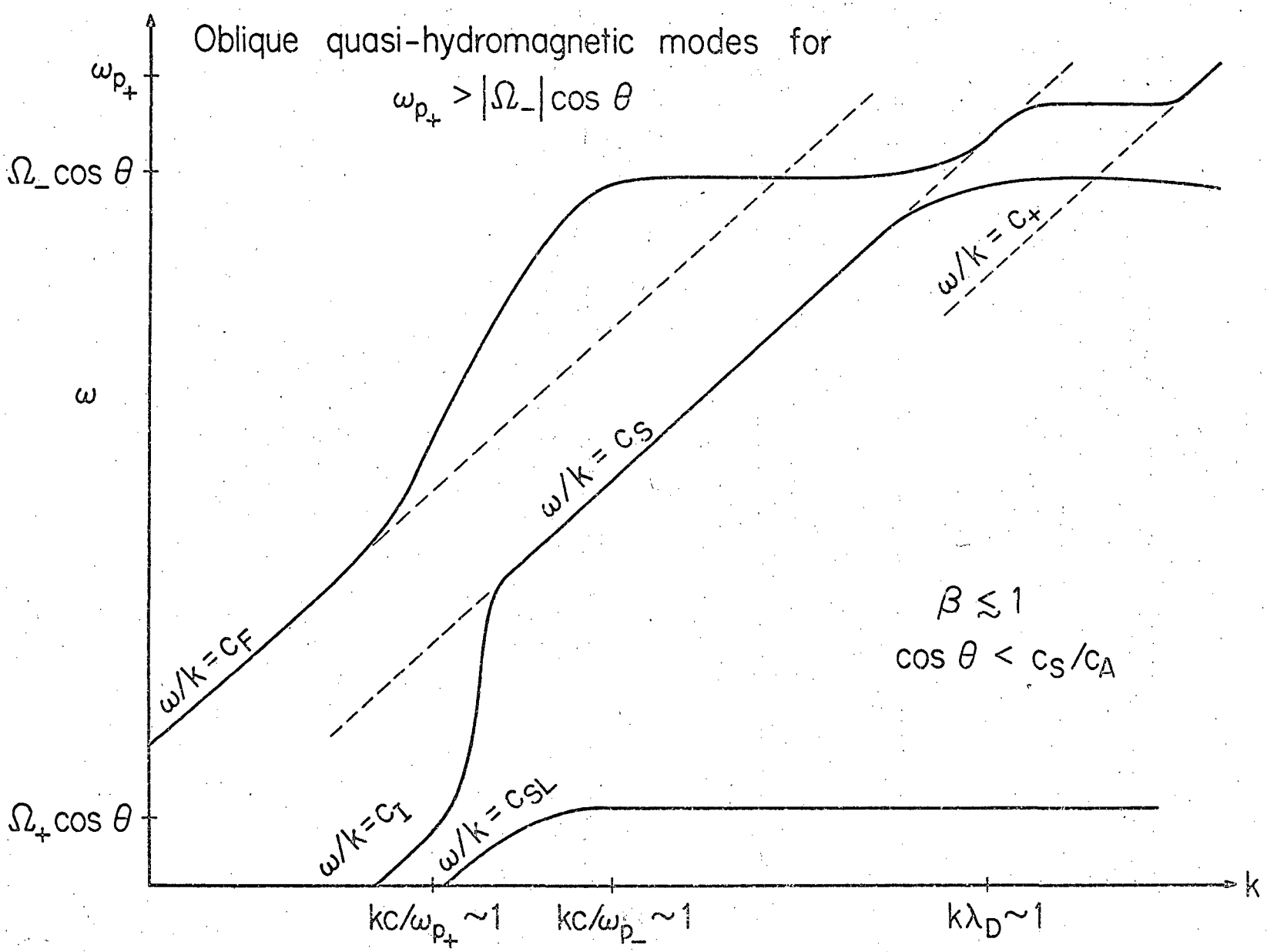
Oblique quasi-hydromagnetic modes for
$\omega_{p_+} > |\Omega_-| \cos\theta$
ω_{p_+}
$\Omega_- \cos\theta$
ω
$\Omega_+ \cos\theta$
$\omega/k = c_F$
$\omega/k = c_I$
$\omega/k = c_{SL}$
$\omega/k = c_S$
$\omega/k = c_+$
$\beta \lesssim 1$
$\cos\theta < c_S/c_A$
$kc/\omega_{p_+} \sim 1$
$kc/\omega_{p_-} \sim 1$
$k\lambda_D \sim 1$
k

Figure 6

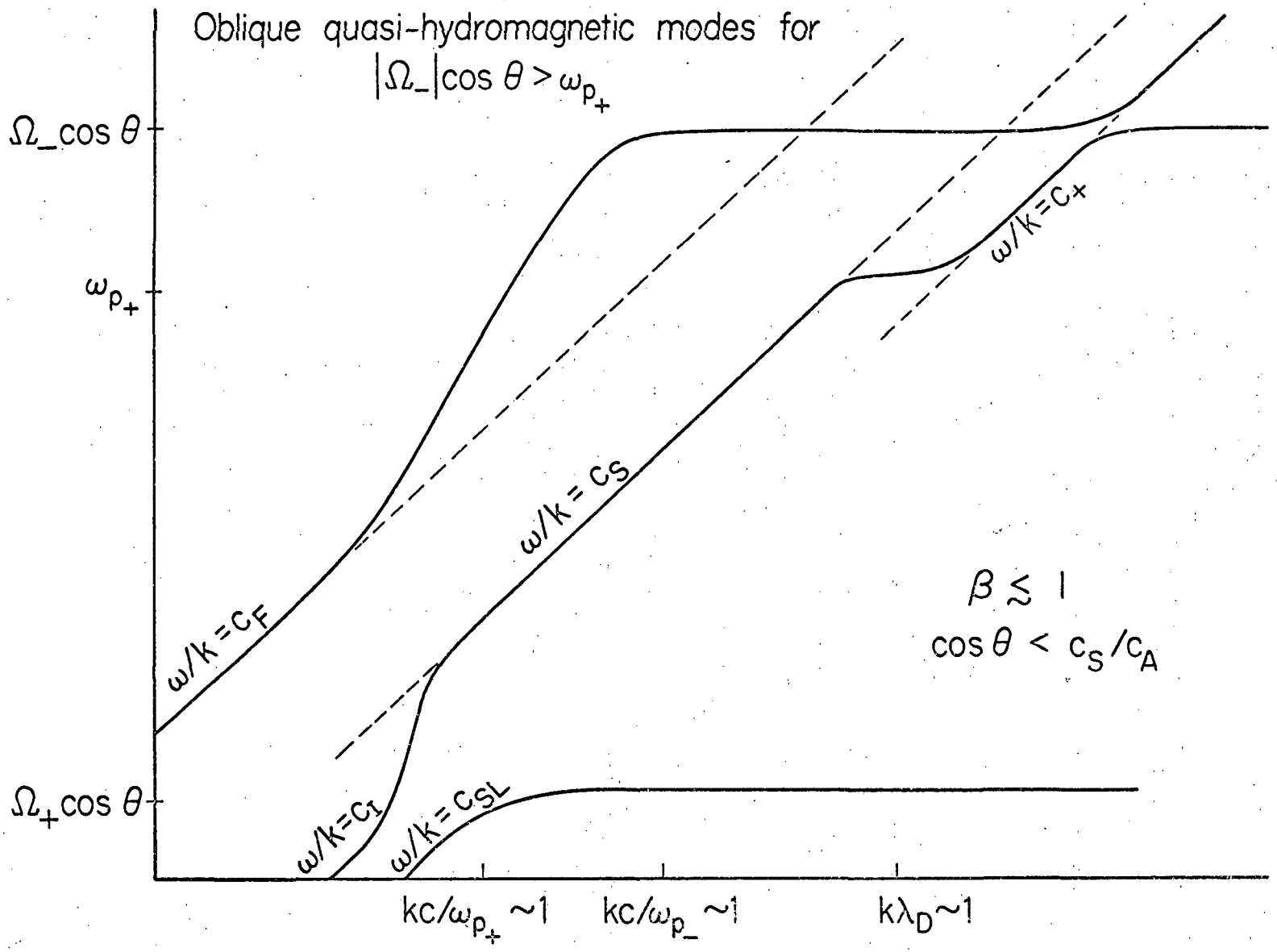
Oblique quasi-hydromagnetic modes for
$|\Omega_-|\cos\theta > \omega_{p_+}$
$\Omega_-\cos\theta$
ω_{p_+}
$\Omega_+\cos\theta$
$\omega/k = c_F$
$\omega/k = c_S$
$\omega/k = c_+$
$\omega/k = c_I$
$\omega/k = c_{SL}$
$\beta \lesssim 1$
$\cos\theta < c_S/c_A$
$kc/\omega_{p_+} \sim 1$
$kc/\omega_{p_-} \sim 1$
$k\lambda_D \sim 1$

Figure 7

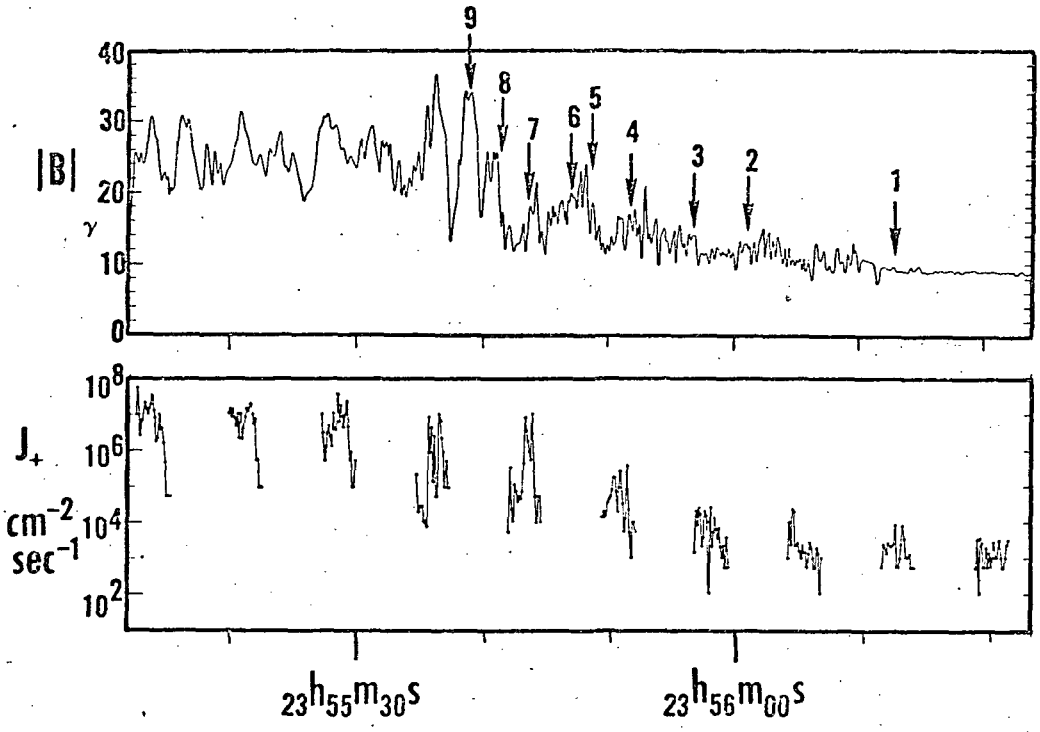
9
8
7
6
5
4
3
2
1
40
30
20
10
0
|B|
γ
10^8
10^6
10^4
10^2
J_+
cm^{-2} sec^{-1}
$23^h55^m30^s$
$23^h56^m00^s$

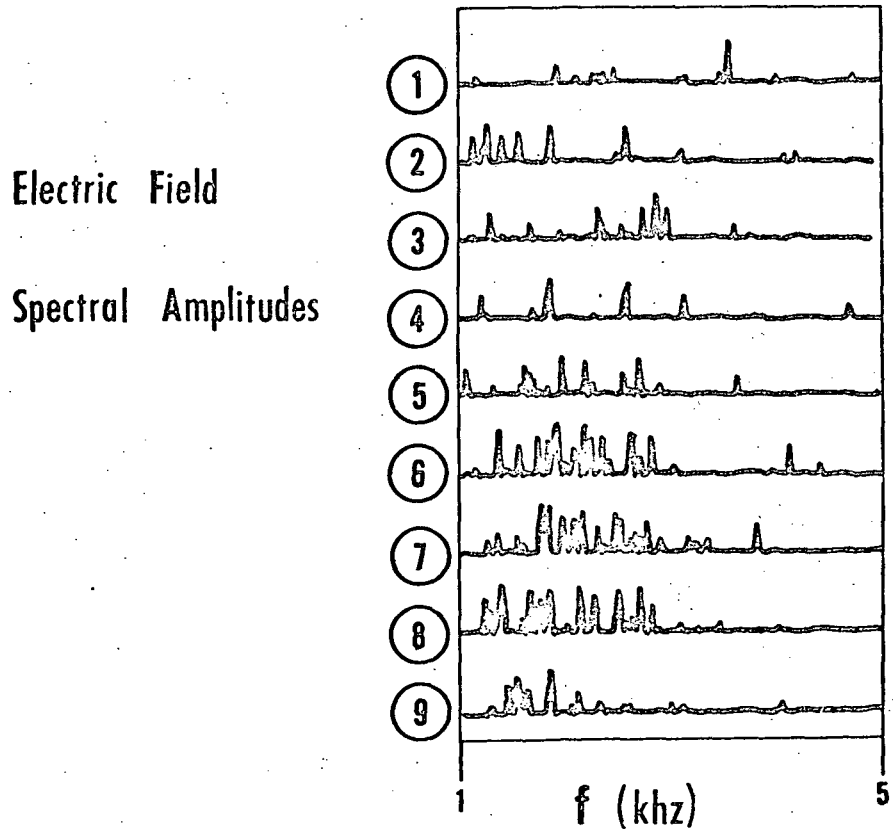
Electric Field
Spectral Amplitudes
1
2
3
4
5
6
7
8
9
1
f (khz)
5

Figure 8